Liquid ^{4}He near the superfluid transition in the presence of a heat current and gravity

Rudolf Haussmann

Sektion Physik, Universität München, Theresienstrasse 37, D-80333 München, Germany

The effects of a heat current and gravity in liquid ^{4}He near the superfluid transition are investigated for temperatures above and below T_λ. We present a renormalization-group calculation based on model F for the Green's function in a self-consistent approximation which in quantum many-particle theory is known as the Hartree approximation. The approach can handle the average order parameter $\langle\psi\rangle=0$ above and below T_λ and includes effects of vortices. We calculate the thermal conductivity $\lambda_T(\Delta T,Q)$ and the specific heat $C(\Delta T,Q)$ for all temperature differences $\Delta T=T-T_\lambda$ and heat currents Q in the critical regime. Furthermore, we calculate the temperature profile $T(z)$. Below T_λ we find a second correlation length $\xi_1\sim Q^{-1}(T_\lambda-T)^{+\nu}$ which describes the dephasing of the order-parameter field due to vortices. We find dissipation and mutual friction of the superfluid–normal-fluid counterflow and calculate the Gorter-Mellink coefficient A. We compare our theoretical results with recent experiments. [S0163-1829(99)04641-X]

I. INTRODUCTION

Gravity and a heat current Q are two sources which influence the superfluid transition of liquid ^{4}He at $T_\lambda\approx2$ K and cause inhomogeneities in the system. On earth gravity implies a pressure variation $P=P(z)$ where z is the altitude coordinate. Since the superfluid transition temperature $T_\lambda=T_\lambda(P)$ is pressure dependent, $T_\lambda(z)=T_\lambda(P(z))$ depends on the altitude coordinate z with the gradient[1] $\partial T_\lambda/\partial z=+1.273$ μK/cm. On the other hand, a nonzero heat current Q drives the system away from equilibrium. A temperature gradient $\boldsymbol{\nabla}T$ is created which implies that the temperature T is space dependent. We assume that the heat current Q is homogeneous and flows vertically (parallel to the z axis) so that the temperature $T(z)$ depends on the z coordinate only.

The local properties of the system are determined by three parameters, the local temperature difference $\Delta T(z)=T(z)-T_\lambda(z)$, the heat current Q, which is related to $\boldsymbol{\nabla}T$, and gravity g, which is related to $\boldsymbol{\nabla}T_\lambda$. The point $(\Delta T,Q,g)=(0,0,0)$ is a critical point related to the superfluid transition. This means that in thermal equilibrium ($Q=0$) and in microgravity ($g=0$) the system shows a second-order phase transition at $T=T_\lambda$ from the normal-fluid to the superfluid state. Usually, gravity is negligible except for very small heat currents Q and for very small ΔT, i.e., very close to T_λ. Since on earth the gravity acceleration $g=9.81$ m/s^2 is a fixed quantity, in most cases the ΔT-Q plane is considered as the phase diagram.

Liquid ^{4}He close to T_λ in the presence of a heat current Q has been investigated theoretically[2–4] and experimentally.[5–8] In the ΔT-Q plane a line of critical temperatures is found which separates superfluid from normal-fluid helium. A nonzero heat current Q implies that the superfluid transition temperature T_λ is shifted to lower temperatures by $\Delta T_\lambda(Q)$. For small heat currents Q in the critical regime the theory[2,4] predicts the shift $\Delta T_\lambda(Q)\sim-Q^x$ with the exponent $x=1/2\nu=0.745$. In the experiments[5,9–11] a depression $\Delta T_c(Q)$ of the superfluid transition has been observed which agrees qualitatively with the theory, but not quantitatively. For small Q in the critical regime the shift $\Delta T_c(Q)\sim-Q^{0.81}$ has been found.[5] While the exponents do not agree, the experimentally observed shift $\Delta T_c(Q)$ is larger than the theoretically calculated $\Delta T_\lambda(Q)$.

While for $\Delta T\gtrsim\Delta T_\lambda(Q)$ the helium is normal fluid and for $\Delta T\lesssim\Delta T_c(Q)$ it is superfluid, in a recent experiment Liu and Ahlers[6] found a dissipative region for temperatures ΔT in the interval $\Delta T_c(Q)<\Delta T<\Delta T_\lambda(Q)$. This observation indicates that at a finite heat current Q the transition from normal-fluid to superfluid helium may possibly happen in two steps with two transition temperatures $\Delta T_\lambda(Q)$ and $\Delta T_c(Q)$ (relative to the equilibrium transition temperature T_λ). While the upper $\Delta T_\lambda(Q)$ may be identified by the theoretical prediction, the lower $\Delta T_c(Q)$ agrees with the shift of Ref. 5. In a similar experiment performed by Murphy and Meyer[8] also two transition temperatures were found. While the values of $\Delta T_\lambda(Q)$ and $\Delta T_c(Q)$ contain errors, the difference $\Delta T_\lambda(Q)-\Delta T_c(Q)$ is quite well reproduced by the latter experiment.

Heat-transport phenomena in liquid ^{4}He close to T_λ are described by model F of Halperin, Hohenberg, and Siggia[12] which is a model for the critical and hydrodynamic slow variables including fluctuations. Most theoretical investigations are based on this model. In the normal-fluid region for temperatures T above T_λ the heat is transported diffusively driven by the temperature gradient $\boldsymbol{\nabla}T$. In linear response the heat current is $\mathbf{Q}=-\lambda_T\boldsymbol{\nabla}T$ where λ_T is the thermal conductivity. For infinitesimal Q and zero gravity the thermal conductivity λ_T has been calculated within model F in two-loop order.[13] Critical fluctuations, which are taken into account by the renormalization-group (RG) theory, imply a strong enhancement of λ_T close to T_λ. For infinitesimal Q and zero gravity the thermal conductivity λ_T diverges in the limit $T\to T_\lambda$, or more precisely in the limit $(\Delta T,Q,g)\to(0,0,0)$. The RG theory has been extended[3] to calculate λ_T for nonzero heat currents Q but without gravity. It turns out that for finite Q close to T_λ the heat transport becomes nonlinear which means that λ_T becomes Q dependent. It has been shown[3] that λ_T remains finite in this case even for $T=T_\lambda$.

On the other hand, in the superfluid region where $\Delta T(z)$ $< \Delta T_c(Q)$ the heat is transported convectively nearly without friction according to the two-fluid model[14] by the superfluid–normal-fluid counterflow. In this case the temperature gradient ∇T is nearly zero indicating a nearly infinite thermal conductivity λ_T. Mutual friction between the superfluid and the normal-fluid component and dissipation of the heat current occur only by creation of vortices, which, however, is a small effect. Nevertheless, mutual friction in the superfluid state has been measured as early as 1949 by Gorter and Mellink.[15] For the mutual friction force the ansatz $f = A \rho_n \rho_s (v_s - v_n)^3$ was made[15] with a temperature-dependent coefficient A, the so-called Gorter-Mellink coefficient. This ansatz is related to a turbulent superfluid flow[16] and implies a temperature gradient $\nabla T \sim -Q^3$, so that the thermal conductivity is $\lambda_T \sim Q^{-2}$. More recently, the temperature gradient ∇T due to mutual friction in superfluid ^{4}He was measured directly by Baddar et al.[17] in the critical regime close to T_λ. This experiment confirms the ansatz by Gorter and Mellink qualitatively but with a slightly different exponent in the Q dependence or $v_s - v_n$ dependence.

In the intermediate region a crossover between the two heat-transport mechanisms happens. Since the system is spatially inhomogeneous this crossover happens also spatially and implies an interface between superfluid and normal-fluid helium located at a certain z_0. Onuki[2] investigated this interface by solving the model-F equations in mean-field approximation, where critical fluctuations are taken into account by scaling theory. He calculated the temperature profile $T(z)$ and the order-parameter profile $\psi(z)$. While in the normal-fluid region the temperature profile has a finite gradient related to a finite thermal conductivity λ_T, in the superfluid region the temperature profile is absolutely flat and the gradient is zero, so that mutual friction is not included and λ_T is infinite.

The previous RG theories[3,4] were constructed as perturbation theories starting with mean-field solutions of the model F equations. While in the normal-fluid region it is[3] $\langle \psi \rangle = 0$, in the superfluid region a plane-wave order parameter $\langle \psi \rangle = \eta e^{ikz}$ was assumed.[4] Consequently, the temperature profile was found to be flat in the superfluid region so that mutual friction and dissipation by vortex creation are not included in the previous RG theories. In this paper we extend the RG theory in two respects. First, we include gravity. Second, we include mutual friction and dissipation in the superfluid region.

Strong fluctuations of the phase of the order-parameter field ψ can imply that the average order parameter is $\langle \psi \rangle = 0$ even below T_λ. This fact is well known for systems of finite size. Here for nonzero Q the vortices cause sufficiently strong phase fluctuations so that $\langle \psi \rangle = 0$ not only above but also below T_λ. For this reason, in the nonequilibrium state with a nonzero heat current Q we may not start a perturbation theory with a nonzero mean-field order parameter which implies a nonzero $\langle \psi \rangle$. Rather we need a new approach which can handle $\langle \psi \rangle = 0$ above and below T_λ. In this paper we present a self-consistent approximation for the Green's function which can do this and which in quantum many-particle theory is known as the Hartree approximation.[18]

The paper is organized as follows. In Sec. II we describe the model and the necessary field theoretic tools, i.e., the

Feynman rules. In Sec. III the idea of our approach and the calculations of the Green's function and the effective parameters are presented. The renormalization-group theory is applied in Sec. IV to include the critical fluctuations. The thermal conductivity and the temperature profile are calculated in Secs. V and VI, while in Secs. VII and VIII the correlation lengths, the entropy, and the specific heat are considered. We compare our results with experiments and investigate the influence of gravity. In Sec. IX we discuss dissipation and mutual friction for superfluid helium below T_λ. We show that our approach reproduces the ansatz of Gorter and Mellink[15] for the mutual friction force and calculate the Gorter-Mellink coefficient A. The idea of the approach and part of the results have been published already.[19]

II. THE MODEL AND FEYNMAN RULES

Dynamic critical and heat transport phenomena in liquid ^{4}He close to T_λ are well described by model F which is given[12] by the Langevin equations for the order parameter $\psi(\mathbf{r},t)$ and the entropy variable $m(\mathbf{r},t)$:

$$\frac{\partial \psi}{\partial t} = -2\Gamma_0 \frac{\delta H}{\delta \psi^*} + i g_0 \psi \frac{\delta H}{\delta m} + \theta_\psi, \tag{2.1}$$

$$\frac{\partial m}{\partial t} = \lambda_0 \nabla^2 \frac{\delta H}{\delta m} - 2 g_0 \text{Im}\left(\psi^* \frac{\delta H}{\delta \psi^*} \right) + \theta_m, \tag{2.2}$$

where

$$H = \int d^d r \left[\tfrac{1}{2} \tau_0(z) |\psi|^2 + \tfrac{1}{2} |\nabla \psi|^2 + \tilde{u}_0 |\psi|^4 + \tfrac{1}{2} \chi_0^{-1} m^2 \right.$$
$$\left. + \gamma_0 m |\psi|^2 - h_0 m \right] \tag{2.3}$$

is the free-energy functional and θ_ψ and θ_m are Gaussian stochastic forces which incorporate the fluctuations. The heat current Q is imposed by boundary conditions. The gravity is included via the temperature parameter $\tau_0(z)$ in Eq. (2.3) which is related to $T_\lambda(z)$ and depends linearly on the altitude z. Usually, the model is treated by field-theoretic means. The perturbation theory in terms of Feynman diagrams is generated by the Janssen-De Dominicis functional integral[20]

$$Z = \int D\psi D\tilde{\psi} Dm D\tilde{m} \exp\{J\} \tag{2.4}$$

with the functional

$$J = \int d^d r \int dt \left\{ \lambda_0 (\nabla \tilde{m})^2 + \Gamma_0' |\tilde{\psi}|^2 \right.$$
$$- \frac{1}{2} \tilde{\psi}^* \left[\frac{\partial \psi}{\partial t} + 2\Gamma_0 \frac{\delta H}{\delta \psi^*} - i g_0 \psi \frac{\delta H}{\delta m} \right]$$
$$- \frac{1}{2} \tilde{\psi} \left[\frac{\partial \psi^*}{\partial t} + 2\Gamma_0^* \frac{\delta H}{\delta \psi} + i g_0 \psi^* \frac{\delta H}{\delta m} \right]$$
$$\left. - \tilde{m} \left[\frac{\partial m}{\partial t} - \lambda_0 \nabla^2 \frac{\delta H}{\delta m} + 2 g_0 \text{Im}\left(\psi^* \frac{\delta H}{\delta \psi^*} \right) \right] \right\}. \tag{2.5}$$

Here $\tilde{\psi}$ and $\tilde{m}$ are auxiliary fields[21] which are needed for a proper construction of the perturbation theory. While in the

previous theories[3,4] only the free Green's functions were needed, here we will evaluate the self-energy in leading order. For this reason, we briefly describe the Feynman rules by which the diagrams and the terms of the perturbation series are constructed. We decompose the fields into a mean field and a fluctuating contribution according to $\psi = \psi_{mf} + \delta\psi$ and $m = m_{mf} + \delta m$ where ψ_{mf} and m_{mf} are solutions of the model-F equations (2.1) and (2.2) without the stochastic forces. Here we assume a zero mean-field order parameter $\psi_{mf} = 0$ above and below T_λ, so that $\psi = \delta\psi$. The boundary conditions, which imply the heat current, require

$$m_{mf}(z) = -q(\chi_0/\lambda_0)(z - z_0), \qquad (2.6)$$

where q is the entropy current related to the heat current Q in physical units by $q = Q/k_B T_\lambda$. We decompose the functional J in powers of the fluctuating fields according to

$$J = J_2 + J_3 + J_4. \qquad (2.7)$$

The quadratic term is given by

$$J_2 = \int d^d r \int dt [\lambda_0 (\nabla\tilde{m})^2 + \Gamma_0' |\tilde{\psi}|^2$$

$$-\tfrac{1}{2}\tilde{\psi}^* L_0 \psi - \tfrac{1}{2}\psi^* L_0^+ \tilde{\psi} - \tilde{m} N_0 \delta m] \qquad (2.8)$$

with the differential operators

$$L_0 = \partial_t + \Gamma_0 [\tau_0(z) - \nabla^2 + 2\gamma_0 m_{mf}(z)]$$

$$- i(g_0/\chi_0)[m_{mf}(z) - \chi_0 h_0] \qquad (2.9)$$

and

$$N_0 = \partial_t - (\lambda_0/\chi_0)\nabla^2. \qquad (2.10)$$

The third- and fourth-order terms are given by

$$J_3 = \int d^d r \int dt \{\tilde{m}[\lambda_0\gamma_0\nabla^2(\psi^*\psi) + g_0\nabla \operatorname{Im}(\psi^*\nabla\psi)]$$

$$- b_3 \delta m \tilde{\psi}^*\psi - b_3^* \delta m \psi^*\tilde{\psi}\} \qquad (2.11)$$

and

$$J_4 = \int d^d r \int dt \{-b_4\tilde{\psi}^*\psi^*\psi\psi - b_4^*\psi^*\psi^*\psi\tilde{\psi}\}, \qquad (2.12)$$

respectively, where

$$b_3 = \Gamma_0\gamma_0 - ig_0/2\chi_0, \quad b_4 = 2\Gamma_0\tilde{u}_0 - ig_0\gamma_0/2 \quad (2.13)$$

are complex parameters. While the free Green's functions are obtained from the quadratic term J_2, the interaction vertices are obtained from J_3 and J_4. In order to obtain a compact notation of the Feynman rules we combine the fields into vectors

$$(\Psi_\alpha) = \begin{pmatrix} \tilde{\psi} \\ \psi \end{pmatrix}, \quad (M_\alpha) = \begin{pmatrix} \tilde{m} \\ \delta m \end{pmatrix}, \qquad (2.14)$$

where the index $\alpha = 1,2$ distinguishes between fields with and without tilde. Then the several contributions of the functional J can be written as
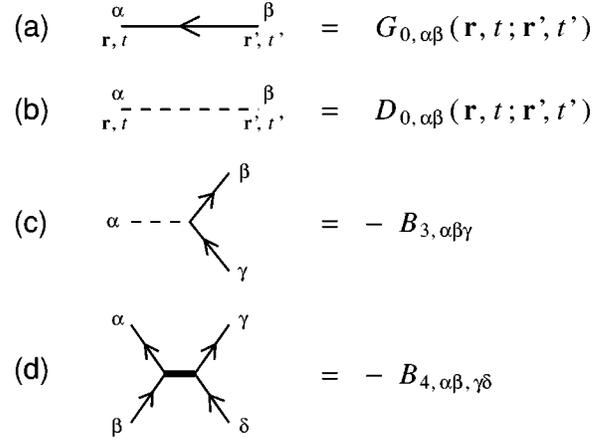

FIG. 1. The elements for constructing the Feynman diagrams: (a) free ψ-field Green's function, (b) free m-field Green's function, (c) three vertex, and (d) four vertex.

$$J_2 = -\int d^d r \int dt [\Psi_\alpha^* K_{0,\alpha\beta}\Psi_\beta + \tfrac{1}{2}M_\alpha E_{0,\alpha\beta}M_\beta],$$

$$(2.15)$$

$$J_3 = -\int d^d r \int dt\, B_{3,\alpha\beta\gamma}M_\alpha\Psi_\beta^*\Psi_\gamma, \qquad (2.16)$$

$$J_4 = -\tfrac{1}{2}\int d^d r \int dt\, B_{4,\alpha\beta,\gamma\delta}(\Psi_\alpha^*\Psi_\beta)(\Psi_\gamma^*\Psi_\delta). \qquad (2.17)$$

Here

$$(K_{0,\alpha\beta}) = \begin{pmatrix} -\Gamma_0' & \tfrac{1}{2}L_0 \\ \tfrac{1}{2}L_0^+ & 0 \end{pmatrix}, \qquad (2.18)$$

$$(E_{0,\alpha\beta}) = \begin{pmatrix} 2\lambda_0\nabla^2 & N_0 \\ N_0^+ & 0 \end{pmatrix} \qquad (2.19)$$

are 2×2 matrices with differential operators as the elements. The free Green's functions are obtained by inverting these matrices according to

$$G_{0,\alpha\beta}(\mathbf{r},t;\mathbf{r}',t') = \langle\Psi_\alpha(\mathbf{r},t)\Psi_\beta^*(\mathbf{r}',t')\rangle_0$$

$$= K_{0,\alpha\beta}^{-1}\delta(\mathbf{r}-\mathbf{r}')\delta(t-t'), \qquad (2.20)$$

$$D_{0,\alpha\beta}(\mathbf{r},t;\mathbf{r}',t') = \langle M_\alpha(\mathbf{r},t)M_\beta(\mathbf{r}',t')\rangle_0$$

$$= E_{0,\alpha\beta}^{-1}\delta(\mathbf{r}-\mathbf{r}')\delta(t-t'). \qquad (2.21)$$

The higher rank tensors $B_{3,\alpha\beta\gamma}$ and $B_{4,\alpha\beta,\gamma\delta}$, which describe the interactions between the fields, are obtained by comparing Eqs. (2.16) and (2.17) with Eqs. (2.11) and (2.12), respectively. While $B_{3,\alpha\beta\gamma}$ contains differential operators, $B_{4,\alpha\beta,\gamma\delta}$ is symmetrized with respect to interchange of the index pairs (α,β) and (γ,δ).

Now, from Eqs. (2.15)–(2.21) the Feynman rules are obtained easily. In Fig. 1 the elements for constructing the Feynman diagrams are shown. The free ψ-field Green's function $G_{0,\alpha\beta}(\mathbf{r},t;\mathbf{r}',t')$ is identified by a directed solid line

[Fig. 1(a)]. The free m-field Green's function $D_{0,\alpha\beta}(\mathbf{r},t;\mathbf{r}',t')$ is identified by a dashed line [Fig. 1(b)]. The m field interacts with the ψ fields by the three vertex shown in Fig. 1(c). Furthermore, the ψ fields interact with each other by the four vertex shown in Fig. 1(d). For each three or four vertex an integration $\int d^d r \int dt$ must be performed. Further rules are applied as usual in field theory. The perturbation series is obtained as the sum of all possible Feynman diagrams which can be constructed from the elements shown in Fig. 1.

III. THE UNRENORMALIZED GREEN'S FUNCTION IN HARTREE APPROXIMATION

To obtain physical quantities we must first calculate the ψ-field Green's function which is defined by

$$G_{\alpha\beta}(\mathbf{r},t;\mathbf{r}',t') = \langle \Psi_\alpha(\mathbf{r},t)\Psi_\beta^*(\mathbf{r}',t') \rangle. \qquad (3.1)$$

This Green's function can be expressed via the Dyson equation

$$G^{-1} = G_0^{-1} - \Sigma \qquad (3.2)$$

in terms of the self-energy $\Sigma_{\alpha\beta}(\mathbf{r},t;\mathbf{r}',t')$. The perturbation series of the self-energy is given by the sum of all irreducible Feynman diagrams with two amputated external solid lines which do not fall into pieces if any internal solid line is cut. A similar Dyson equation exists also for the m-field Green's function $D_{\alpha\beta}(\mathbf{r},t;\mathbf{r}',t')$. However, for our calculations we do not need the latter Green's function explicitly.

In order to account for effects beyond the perturbation theory we must resum the Feynman diagrams partially in an appropriate way. In the critical regime close to a second-order phase transition, infrared singularities occur which must be resummed by renormalization and application of the renormalization-group theory. For model F the RG theory was elaborated up to two-loop order by Dohm.[13] All the renormalized coupling parameters depending on a RG flow parameter were determined[13] by adjusting the superfluid density, the specific heat, and the thermal conductivity to the respective experimental data. Thus model F can be used for explicit calculations of physical quantities in the critical regime near T_λ without any (further) adjustable parameters.

Here we first apply an additional resummation which is well known in quantum many-particle physics.[22–24] We resum with respect to all self-energy subdiagrams so that the perturbation series becomes self-consistent with respect to the ψ-field Green's function G. This means that now the solid lines are thick and identified by the exact Green's function G as shown in Fig. 2(a). To avoid multiple counting of diagrams, only the irreducible diagrams are included in the perturbation series, which do not contain self-energy subdiagrams or equivalently which do not fall into pieces if any two of the internal thick solid lines are cut. The resummation was used first by Luttinger and Ward[22] and was formulated in terms of a Legendre transformation by De Dominicis and Martin.[23] By truncating the self-consistent perturbation series of the self-energy Σ the conserving approximation of Baym and Kadanoff[25,26] is obtained.

Here, we approximate the self-energy Σ by including only the tadpole diagrams as shown in Fig. 2(b). This approxima-

FIG. 2. (a) The exact ψ-field Green's function is identified by a thick solid directed line. (b) The self-energy in Hartree approximation.

tion is equivalent to the Hartree approximation in quantum mechanics.[18] The Dyson equation (3.2) together with the self-energy in Fig. 2(b) are self-consistent equations which enable an explicit calculation of the unrenormalized Green's function G. However, since we consider liquid ^{4}He in the critical regime near T_λ, a second resummation is necessary: the self-consistent perturbation series and hence the Hartree approximation must be modified by renormalization and application of the RG theory.

We have several reasons to believe that the Hartree approximation combined with the RG theory is successful for model F above and below T_λ where the order parameter is always $\langle\psi\rangle = 0$. Moreover, we will show that the approximation includes vortices and mutual friction so that it may be a possible approach to describe the dissipation in the superfluid state observed in the experiments.[6,17] First of all, if we generalize model F by replacing the complex field ψ by a vector $\Psi = (\psi_1, \ldots, \psi_n)$ of n complex fields, then it turns out that the Hartree approximation is exact for the Green's function G in the limit $n\to\infty$. For each closed loop of thick solid lines there will be a factor n. If we rescale the coupling parameters according to $\tilde{u}_0 \sim n^{-1}$, $\gamma_0 \sim n^{-1/2}$, and $g_0 \sim n^{-1/2}$ so that $B_{3,\alpha\beta\gamma} \sim n^{-1/2}$ and $B_{4,\alpha\beta,\gamma\delta} \sim n^{-1}$, then only the tadpole diagrams shown in Fig. 2(b) will be nonzero in the limit $n\to\infty$. It is well known that models involving Ginzburg-Landau functionals like the ϕ^4 model can be solved exactly in this limit (see, e.g., Ref. 27). The same is true also for model F. While in the limit $n\to\infty$ the RG theory is not needed because the Hartree approximation is exact, in our case for $n=1$ the RG theory is necessary to obtain the correct critical behavior of the physical quantities near T_λ.

We may expect that beyond the Hartree approximation an $1/n$ expansion may yield the proper corrections. However, this is not true. By experience with quantum-field theory of many-particle systems with degeneracies[28,29] we have found that proper corrections are given by the modified self-consistent random-phase approximation (modified SC-RPA), where the modification is a gauge transformation which implies bosonization for a proper treatment of the low energetic collective excitations. The method has been invented for two-dimensional electron systems in the regime of the fractional quantum Hall effect[28] and tested for simple exactly solvable models.[29] We have found that the modified SC-RPA can describe the superfluid transition and Bose-Einstein condensation in interacting boson systems where the average order parameter is $\langle\psi\rangle = 0$ due to phase fluctuations above and below the transition.[29] For this reason we believe that the modified SC-RPA combined with the RG theory will be successful in the present case for model F.

The main feature of the modified SC-RPA is that it implies a nontrivial spectrum for the Green's function G while the Hartree approximation does not. This fact is important in quantum many-particle physics because the spectra of the quasiparticles are important physical results. However, in the present case for critical phenomena and second-order phase transitions nontrivial spectra are not essential while the application of the RG theory is important. For this reason, the Hartree approximation combined with the RG theory should be sufficient for our purposes. Even though the modified SC-RPA combined with the RG theory would be desirable, we expect only some corrections while the calculations would be much more complicated.

A. Evaluation of the Green's function

Now, we evaluate the self-energy Σ and determine the unrenormalized Green's function G in Hartree approximation. The tadpole diagrams in Fig. 2(b) imply a self energy of the form

$$\Sigma_{\alpha\beta}(\mathbf{r},t;\mathbf{r}',t')=-\Delta K_{\alpha\beta}\delta(\mathbf{r}-\mathbf{r}')\delta(t-t'), \quad (3.3)$$

where $\Delta K_{\alpha\beta}$ are the elements of a 2×2 matrix which depend on the space coordinate z but do not contain differential operators. Applying the Feynman rules of Sec. II we obtain the matrix

$$(\Delta K_{\alpha\beta})=\begin{pmatrix} 0 & \frac{1}{2}\Delta L \\ \frac{1}{2}\Delta L^+ & 0 \end{pmatrix}, \quad (3.4)$$

where

$$\Delta L=2b_3 N_0^{-1}[\lambda_0\gamma_0\boldsymbol{\nabla}^2 n_{\mathrm{s}}+g_0\boldsymbol{\nabla}\mathbf{J}_{\mathrm{s}}]+2b_4 n_{\mathrm{s}}. \quad (3.5)$$

Here

$$n_{\mathrm{s}}=\langle|\psi|^2\rangle=G_{22}(\mathbf{r},t;\mathbf{r},t) \quad (3.6)$$

is a density related to the entropy and

$$\mathbf{J}_{\mathrm{s}}=\langle\mathrm{Im}[\psi^*\boldsymbol{\nabla}\psi]\rangle=\lim_{\mathbf{r}'\to\mathbf{r}}\mathrm{Im}[\boldsymbol{\nabla}G_{22}(\mathbf{r},t;\mathbf{r}',t)] \quad (3.7)$$

is the superfluid current density. N_0^{-1} is the inverse of the differential operator (2.10). Since n_{s} and $\mathbf{J}_{\mathrm{s}}$ in Eq. (3.5) depend only on z, we may drop the time derivative in N_0^{-1}. Then, from Eq. (3.5) we obtain

$$\Delta L=2(b_4-\chi_0\gamma_0 b_3)n_{\mathrm{s}}-2b_3(\chi_0 g_0/\lambda_0)(\boldsymbol{\nabla}^2)^{-1}(\boldsymbol{\nabla}\mathbf{J}_{\mathrm{s}}). \quad (3.8)$$

Inserting b_3 and b_4 of Eq. (2.13) we obtain

$$b_4-\chi_0\gamma_0 b_3=2\Gamma_0(\tilde{u}_0-\tfrac{1}{2}\chi_0\gamma_0^2)=2\Gamma_0 u_0, \quad (3.9)$$

where $u_0=\tilde{u}_0-\tfrac{1}{2}\chi_0\gamma_0^2$ is the effective coupling between the ψ fields in thermal equilibrium after the entropy field m has been integrated out (see Ref. 13). Since the heat current Q flows in z direction, only the z component $J_{\mathrm{s},z}=J_{\mathrm{s}}$ of the superfluid current is nonzero so that

$$(\boldsymbol{\nabla}^2)^{-1}(\boldsymbol{\nabla}\mathbf{J}_{\mathrm{s}})=\partial_z^{-1}J_{\mathrm{s}}. \quad (3.10)$$

Thus from Eq. (3.8) we obtain

$$\Delta L=\Gamma_0[4u_0 n_{\mathrm{s}}-2\chi_0\gamma_0(g_0/\lambda_0)\partial_z^{-1}J_{\mathrm{s}}]+ig_0(g_0/\lambda_0)\partial_z^{-1}J_{\mathrm{s}}. \quad (3.11)$$

Now, we define

$$L=L_0+\Delta L. \quad (3.12)$$

Then from Eqs. (2.9) and (3.11) we obtain

$$L=\partial_t+\Gamma_0[r_1(z)-\boldsymbol{\nabla}^2]-i\frac{g_0}{2\chi_0\gamma_0}\Delta r_0(z), \quad (3.13)$$

where

$$r_1(z)=\tau_0(z)+2\chi_0\gamma_0\left[\frac{1}{\chi_0}m_{\mathrm{mf}}(z)-\frac{g_0}{\lambda_0}\partial_z^{-1}J_{\mathrm{s}}\right]+4u_0 n_{\mathrm{s}} \quad (3.14)$$

and

$$\Delta r_0(z)=2\chi_0\gamma_0\left[\frac{1}{\chi_0}m_{\mathrm{mf}}(z)-h_0-\frac{g_0}{\lambda_0}\partial_z^{-1}J_{\mathrm{s}}\right] \quad (3.15)$$

are effective parameters. Furthermore, we define the matrix

$$K_{\alpha\beta}=K_{0,\alpha\beta}+\Delta K_{\alpha\beta} \quad (3.16)$$

and obtain

$$(K_{\alpha\beta})=\begin{pmatrix} -\Gamma_0' & \frac{1}{2}L \\ \frac{1}{2}L^+ & 0 \end{pmatrix}. \quad (3.17)$$

Now, the Green's function G in Hartree approximation is obtained easily. We find that Eqs. (3.12) and (3.16) are equivalent to the Dyson equation (3.2). Thus as a result we obtain

$$G_{\alpha\beta}(\mathbf{r},t;\mathbf{r}',t')=K_{\alpha\beta}^{-1}\delta(\mathbf{r}-\mathbf{r}')\delta(t-t'), \quad (3.18)$$

where $K_{\alpha\beta}$ is given by Eq. (3.17) together with Eq. (3.13). Clearly, the Green's function G in Hartree approximation has the same structure as the free Green's function G_0 where just the parameters have been replaced by effective parameters. As a consequence, the following calculations are considerably simplified because we may restrict the considerations to the effective parameters $r_1(z)$ and $\Delta r_0(z)$ only. We will derive self-consistent equations for $r_1(z)$ and $\Delta r_0(z)$ to determine the effective parameters. Eventually, the Green's function G is obtained from Eq. (3.18) together with Eqs. (3.13) and (3.17).

B. Evaluation of n_{s} and J_{s}

Next we evaluate n_{s} and J_{s} by inserting the Green's function (3.18) into Eqs. (3.6) and (3.7). In Ref. 3 n_{s} and J_{s} were evaluated for the free Green's function so that here we need not perform these calculations once again. Since the Green's function in Hartree approximation has the same structure, we may use the results of Ref. 3 with a slight modification. We just need to replace the free parameters by the effective parameters $r_1(z)$ and $\Delta r_0(z)$ appropriately. The basic assumption of the previous calculations[3] was that the parameters

$r_1(z)$ and $\Delta r_0(z)$ in the Green's function are linear functions of z. For the free Green's function, where n_s and J_s in Eqs. (3.14) and (3.15) are omitted, this is indeed true, because $m_{mf}(z)$ defined in Eq. (2.6) and $\tau_0(z)$, which is related to $T_\lambda(z)$, are linear functions of z. Thus in the present case we must assume as an approximation that $r_1(z)$ and $\Delta r_0(z)$ are linearized locally so that only the slopes r_1' and $\Delta r_0'$ are included but the curvatures and the higher-order derivatives are neglected. We will later show in Sec. VII that this assumption is justified.

Now, from Eqs. (3.22) and (3.25) in the second paper of Ref. 3 we obtain

$$n_s = 2 \ \Phi_{-1+\epsilon/2}(X) \int \frac{d^d p}{(2\pi)^d} \frac{1}{r_1(z)+\mathbf{p}^2}, \quad (3.19)$$

and

$$J_s = \frac{g_0}{2\Gamma_0'} \frac{\Delta r_0'}{2\chi_0\gamma_0} \Phi_{\epsilon/2}(X) \int \frac{d^d p}{(2\pi)^d} \frac{1}{[r_1(z)+\mathbf{p}^2]^2}. \quad (3.20)$$

Here ϵ is related to the space dimension d by $\epsilon = 4 - d$. The function $\Phi_\alpha(X)$ is defined by the asymptotic series

$$\Phi_\alpha(X) = \sum_{N=0}^\infty \frac{\Gamma(\alpha+3N)}{\Gamma(\alpha)} \frac{X^N}{N!} \quad (3.21)$$

and contains all the effects beyond linear response theory. In the integrals the parameter $\tilde{r}_0(z)$ of Ref. 3 has been replaced by the effective parameter $r_1(z)$. The dimensionless parameter X is given here by

$$X = \frac{1}{12[r_1(z)]^3} \left[r_1'^2 + 2\frac{\Gamma_0''}{\Gamma_0'}\left(\frac{g_0}{4\chi_0\gamma_0\Gamma_0'}\Delta r_0'\right)r_1' \right.$$
$$\left. - \left(\frac{g_0}{4\chi_0\gamma_0\Gamma_0'}\Delta r_0'\right)^2 \right], \quad (3.22)$$

where

$$r_1' = \partial_z r_1(z), \quad \Delta r_0' = \partial_z \Delta r_0(z). \quad (3.23)$$

The entropy current q in the formulas of Ref. 3 is here replaced by r_1' or $\Delta r_0'$ times $-\lambda_0/2\chi_0\gamma_0$. We note that our formulas reduce to those of Ref. 3 if we omit n_s and J_s in the effective parameters (3.14) and (3.15) and if we neglect gravity. The integrals can be evaluated[3,13] in dimensional regularization so that we obtain

$$n_s(z) = -\frac{2}{\epsilon} A_d \Phi_{-1+\epsilon/2}(X)[r_1(z)]^{1-\epsilon/2}, \quad (3.24)$$

and

$$J_s(z) = \frac{g_0}{2\Gamma_0'} \frac{\Delta r_0'}{2\chi_0\gamma_0} \frac{1}{\epsilon} A_d\left(1 - \frac{\epsilon}{2}\right) \Phi_{\epsilon/2}(X)[r_1(z)]^{-\epsilon/2}, \quad (3.25)$$

where $A_d = S_d \Gamma(1-\epsilon/2)\Gamma(1+\epsilon/2)$, $S_d = \Omega_d/(2\pi)^d$, and $\Omega_d = 2\pi^{d/2}/\Gamma(d/2)$ is the surface of the d-dimensional unit sphere. Clearly, $n_s(z)$ and $J_s(z)$ depend on z implicitly via $r_1(z)$ and the derivatives r_1' and $\Delta r_0'$.

C. Self-consistent equations for the effective parameters

Equations (3.14) and (3.15) together with Eqs. (3.24) and (3.25) are self-consistent equations for the effective parameters $r_1(z)$ and $\Delta r_0(z)$. The structure of these equations can be simplified. First of all we note that the effective parameters and its derivatives can be related to the temperatures $T(z)$, $T_\lambda(z)$, and the heat current Q. We find

$$\Delta r_0(z) = 2\chi_0\gamma_0\left\langle\frac{\delta H}{\delta m}\right\rangle = 2\chi_0\gamma_0 \frac{T(z)-T_0}{T_\lambda}. \quad (3.26)$$

To prove this relation $\langle\delta H/\delta m\rangle$ can be evaluated explicitly in Hartree approximation and compared with Eq. (3.15). Equivalently, we take the average of Eq. (2.2) and obtain $\partial_t\langle m\rangle + \nabla\mathbf{q} = 0$ where $\mathbf{q}$

$$\mathbf{q} = -\lambda_0\nabla\left\langle\frac{\delta H}{\delta m}\right\rangle - g_0\mathbf{J}_s \quad (3.27)$$

is the entropy current. Since z is the only space coordinate, this equation can be rewritten in the form

$$\frac{\partial}{\partial z}\left\langle\frac{\delta H}{\delta m}\right\rangle = -\frac{q}{\lambda_0} - \frac{g_0}{\lambda_0}J_s$$
$$= \frac{\partial}{\partial z}\left[\frac{1}{\chi_0}m_{mf}(z) - h_0 - \frac{g_0}{\lambda_0}\partial_z^{-1}J_s\right]. \quad (3.28)$$

Thus integrating this equation and comparing with Eq. (3.15) we obtain Eq. (3.26). We note that Eq. (3.15) contains integration constants via $m_{mf}(z)$ and $\partial_z^{-1}J_s$. Since m is the entropy density divided by k_B, the quantity $\langle\delta H/\delta m\rangle$ is a temperature difference divided by T_λ. This fact explains the last equality sign in Eq. (3.26). Here T_0 is a constant reference temperature which may be arbitrary. In the denominator the z dependence of T_λ due to gravity is very small and may be neglected.

The temperature parameter $r_0(z)$ is defined by[3]

$$r_0(z) = \tau_0(z) + 2\chi_0\gamma_0\left(h_0 + \left\langle\frac{\delta H}{\delta m}\right\rangle\right)$$
$$= \tau_0(z) + 2\chi_0\gamma_0 h_0 + \Delta r_0(z). \quad (3.29)$$

In thermal equilibrium this parameter is the coefficient of $|\psi|^2$ in the energy functional after the entropy variable m has been integrated out.[13] It is related to the temperature by

$$r_0(z) - r_{0c} = 2\chi_0\gamma_0\frac{T(z)-T_\lambda(z)}{T_\lambda} = 2\chi_0\gamma_0\frac{\Delta T(z)}{T_\lambda}. \quad (3.30)$$

The critical value is $r_{0c} = 0$ in one-loop approximation[13] and hence also in Hartree approximation. We find that the first line on the right-hand side of Eq. (3.14) is identified by $r_0(z)$. Thus Eq. (3.14) simplifies into

$$r_1(z) = r_0(z) + 4u_0 n_s. \quad (3.31)$$

We resolve this equation with respect to $r_0(z)$ and insert Eq. (3.24) for n_s. Then we obtain

$$r_0(z) = r_1(z)\left\{ 1 + \frac{8u_0}{\epsilon} A_d \Phi_{-1+\epsilon/2}(X)[r_1(z)]^{-\epsilon/2} \right\}. \tag{3.32}$$

Next, we take the derivative of this equation with respect to z and obtain

$$r_0' = r_1'\left\{ 1 + \frac{8u_0}{\epsilon} A_d\left(1 - \frac{\epsilon}{2} \right) \Phi_{\epsilon/2}(X)[r_1(z)]^{-\epsilon/2} \right\}. \tag{3.33}$$

Furthermore, the derivative of Eq. (3.15) yields

$$\Delta r_0' = -2\chi_0 \gamma_0 \left[\frac{q}{\lambda_0} + \frac{g_0}{\lambda_0} J_s \right]. \tag{3.34}$$

Resolving this equation with respect to q and inserting Eq. (3.25) for J_s we obtain

$$q = \frac{Q}{k_B T_\lambda} = -\lambda_0 \left\{ 1 + \frac{g_0^2}{2\lambda_0 \Gamma_0'} \frac{1}{\epsilon} A_d \left(1 - \frac{\epsilon}{2} \right) \right.$$
$$\left. \times \Phi_{\epsilon/2}(X)[r_1(z)]^{-\epsilon/2} \right\} \frac{\Delta r_0'}{2\chi_0 \gamma_0}. \tag{3.35}$$

On the other hand, from Eq. (3.26) we find that $\Delta r_0'$ is related to the temperature gradient $\partial_z T$ by

$$\Delta r_0' = 2\chi_0 \gamma_0 T_\lambda^{-1} \partial_z T. \tag{3.36}$$

Finally, Eq. (3.29) implies

$$r_0' = \Delta r_0' - 2\chi_0 \gamma_0 T_\lambda^{-1} \partial_z T_\lambda, \tag{3.37}$$

where we have identified $\tau_0' = -2\chi_0 \gamma_0 T_\lambda^{-1} \partial_z T_\lambda$. Clearly, the difference between r_0' and $\Delta r_0'$ is due to the gradient of $T_\lambda(z)$ which is the effect of gravity. Thus in a microgravity environment r_0' and $\Delta r_0'$ are equal.

Now, the self-consistent equations which allow the determination of all the effective parameters are given by Eqs. (3.32), (3.33), and (3.35) together with Eqs. (3.26), (3.30), (3.37), and (3.22). These are seven equations for seven unknown variables $r_0(z)$, $\Delta r_0(z)$, $r_1(z)$, r_0', $\Delta r_0'$, r_1', and X. As an input we need the temperatures $T(z)$, $T_\lambda(z)$, the difference $\Delta T(z) = T(z) - T_\lambda(z)$, the heat current $Q = k_B T_\lambda q$, and the gradient $\partial_z T_\lambda$ for a given space variable z. Since the seven equations do not depend explicitly on z, we do not need the temperature profiles as functions of z. Instead, we obtain the temperature gradient $\partial_z T$ from Eq. (3.36) so that the temperature profile $T(z)$ can be calculated by integration. Eventually, for given ΔT and Q physical quantities like the specific heat and the thermal conductivity can be calculated. This will be done in Secs. V and VIII.

IV. RENORMALIZATION AND APPLICATION OF THE RENORMALIZATION-GROUP THEORY

In Eqs. (3.32), (3.33), and (3.35) the first-order terms exhibit infrared divergences at criticality where $r_1(z) \to 0$ while the function $\Phi_\alpha(X)$ is of order unity. For this reason the renormalization of these equations and the application of the

RG theory are necessary to achieve a resummation of the infrared divergences and a proper treatment of the critical fluctuations. We use the concept of renormalization by minimal subtraction of dimensional poles. The calculations are performed at fixed dimension $d = 4 - \epsilon$ (i.e., no ϵ expansion is applied). For model F this renormalization scheme is described in Ref. 13. The renormalization factors of the fields ψ and $\tilde{\psi}$ are $Z_\psi = Z_{\tilde{\psi}} = 1$ in one-loop order and hence also in Hartree approximation. Thus the Green's function G is not renormalized here. As a consequence, also the operator L defined in Eq. (3.13) is not renormalized. The parameter Γ_0 is renormalized according to[13] $\Gamma_0 = Z_\Gamma^{-1}\Gamma$ where, however, in one-loop order and in Hartree approximation $Z_\Gamma = 1$. Thus from Eq. (3.13) we conclude that $r_1(z)$ is not renormalized.

The parameters γ_0 and g_0 are renormalized according to[13]

$$\chi_0 \gamma_0 = \gamma(\chi_0 Z_m)^{1/2} Z_r(\mu^\epsilon/A_d)^{1/2}, \tag{4.1}$$

$$g_0 = g(\chi_0 Z_m)^{1/2}(\mu^\epsilon/A_d)^{1/2}. \tag{4.2}$$

Furthermore, we renormalize $\Delta r_0(z) = Z_r \Delta r(z)$. Consequently, we find

$$\frac{g_0}{2\chi_0 \gamma_0} \Delta r_0(z) = \frac{g}{2\gamma} \Delta r(z) \tag{4.3}$$

which is consistent with the requirement that the last term in Eq. (3.13) is not renormalized. Thus in terms of the renormalized parameters the operator (3.13) reads

$$L = \partial_t + \Gamma[r_1(z) - \nabla^2] - i(g/2\gamma)\Delta r(z). \tag{4.4}$$

Next we renormalize Eq. (3.32). For this purpose we need the relations[13]

$$r_0(z) - r_{0c} = Z_r r(z), \tag{4.5}$$

$$u_0 = u Z_u Z_\psi^{-2}(\mu^\epsilon/A_d), \tag{4.6}$$

where $r_{0c} = 0$ and $Z_\psi = 1$ in Hartree approximation. We separate the ultraviolet divergence on the right-hand side of Eq. (3.32) which here in dimensional regularization is a pole $\sim 1/\epsilon$. By choosing

$$Z_r = Z_u = 1/[1 - 8u/\epsilon] \tag{4.7}$$

the ultraviolet divergence is canceled. Eventually we obtain

$$r(z) = r_1(z)\left\{ 1 + \frac{8u}{\epsilon}\left[\Phi_{-1+\epsilon/2}(X)\left(\frac{r_1(z)}{\mu^2} \right)^{-\epsilon/2} - 1 \right] \right\}. \tag{4.8}$$

Analogously we separate the ultraviolet divergence on the right-hand side of Eq. (3.33). Using Eqs. (4.5)–(4.7) we obtain

$$r' = r_1'\left\{ 1 + \frac{8u}{\epsilon}\left[\left(1 - \frac{\epsilon}{2} \right)\Phi_{\epsilon/2}(X)\left(\frac{r_1(z)}{\mu^2} \right)^{-\epsilon/2} - 1 \right] \right\}. \tag{4.9}$$

We replace the parameters in the dimensionless variable X defined in Eq. (3.22) by the renormalized ones. It turns out that all Z factors cancel so that X is not renormalized. Thus we obtain

$$X = \frac{1}{12[r_1(z)]^3}\left[r_1'^2 + 2\frac{\Gamma''}{\Gamma'}\left(\frac{g}{4\gamma\Gamma'}\Delta r'\right)r_1' - \left(\frac{g}{4\gamma\Gamma'}\Delta r'\right)^2\right].$$

(4.10)

For convenience we replace the renormalized couplings by the dimensionless combinations[13] $w = \Gamma/\lambda$, $F = g/\lambda$, and $f = F^2/w'$. Furthermore, we introduce the dimensionless effective parameters

$$\rho = r(z)/\mu^2, \quad \rho' = r'/\mu^3,$$

(4.11)

$$\Delta\rho = \Delta r(z)/\mu^2, \quad \Delta\rho' = \Delta r'/\mu^3,$$

(4.12)

$$\rho_1 = r_1(z)/\mu^2, \quad \rho_1' = r_1'/\mu^3.$$

(4.13)

Since the coordinate z does not appear explicitly in the self-consistent equations for the effective parameters, we omit z as an argument from now on. Then, Eqs. (4.8)–(4.10) can be rewritten as

$$\rho = \rho_1\left\{1 + \frac{8u}{\epsilon}[\Phi_{-1+\epsilon/2}(X)\rho_1^{-\epsilon/2} - 1]\right\},$$

(4.14)

$$\rho' = \rho_1'\left\{1 + \frac{8u}{\epsilon}\left[\left(1 - \frac{\epsilon}{2}\right)\Phi_{\epsilon/2}(X)\rho_1^{-\epsilon/2} - 1\right]\right\},$$

(4.15)

$$X = \frac{1}{12\rho_1^3}\left[\rho_1'^2 + 2\frac{w''}{w'}\left(\frac{F}{4\gamma w'}\Delta\rho'\right)\rho_1' - \left(\frac{F}{4\gamma w'}\Delta\rho'\right)^2\right],$$

(4.16)

respectively.

The entropy current is renormalized by[3]

$$q = (\chi_0 Z_m)^{1/2}q^{\text{ren}}.$$

(4.17)

This equation together with Eq. (4.2) implies that the ratio

$$Q/g_0 k_B T_\lambda = q/g_0 = (q^{\text{ren}}/g)(A_d/\mu^\epsilon)^{1/2}$$

(4.18)

need not be renormalized because the Z factors cancel. In Eq. (3.35) we separate the ultraviolet divergence and replace the coupling parameters by the renormalized parameters. Additionally, we need the renormalization[13] $\lambda_0 = \chi_0 Z_\lambda^{-1}\lambda$. Using the Z factor product

$$Z_m Z_\lambda = 1/[1 - f/2\epsilon]$$

(4.19)

we find that the ultraviolet divergence is canceled. Then, in terms of the renormalized couplings and effective parameters we obtain

$$\frac{Q\mu^{\epsilon-3}}{g_0 k_B T_\lambda} = -\frac{A_d}{2\gamma F}\left\{1 + \frac{f}{2\epsilon}\left[\left(1 - \frac{\epsilon}{2}\right)\Phi_{\epsilon/2}(X)\rho_1^{-\epsilon/2} - 1\right]\right\}\Delta\rho',$$

(4.20)

where the left-hand side need not be renormalized because of Eq. (4.18). Finally, we renormalize Eqs. (3.26), (3.30), (3.36), and (3.37) and obtain

$$\Delta\rho = \tau^{-1}[T(z) - T_0]/T_\lambda,$$

(4.21)

$$\rho = \tau^{-1}[T(z) - T_\lambda(z)]/T_\lambda,$$

(4.22)

$$\Delta\rho' = \tau^{-1}(\mu T_\lambda)^{-1}\partial_z T,$$

(4.23)

$$\rho' = \Delta\rho' - \tau^{-1}(\mu T_\lambda)^{-1}\partial_z T_\lambda,$$

(4.24)

respectively, where

$$\tau = \left(\frac{A_d\mu^d}{\chi_0 Z_m}\right)^{1/2}\frac{1}{2\gamma}.$$

(4.25)

In these equations Z_m does not cancel. We note that the renormalization is exact in all the above equations. This means that we need not expand the Z factors in powers of the renormalized couplings. The reason of this fact is that the Hartree approximation is exact in the limit $n\to\infty$ for model F with an n-component complex order parameter. On the other hand, the Z factors do not agree with those of the previous theories[13] in one loop-order because the Hartree approximation is not a loop expansion. (The correct one-loop Z factors would be obtained if we would consider a Hartree-Fock approximation and include both the Hartree and the Fock term in the self-energy Σ.)

By the renormalization a characteristic length scale is introduced which is described by the parameter μ. The RG theory is based on the fact that this length scale is arbitrary and may be changed according to $\mu\to\mu l$, where l is the RG flow parameter. As a consequence, the renormalized coupling parameters $u(l)$, $\gamma(l)$, $w(l)$, $F(l)$, and $f(l)$ depend on l. Furthermore, also the Z factors depend on l. Now, the dimensionless parameter defined in Eq. (4.25) reads

$$\tau = \left(\frac{A_d(\mu l)^d}{\chi_0 Z_m(l)}\right)^{1/2}\frac{1}{2\gamma(l)}.$$

(4.26)

For convenience we will use τ as the RG flow parameter instead of l because τ is closely related to the reduced temperature by Eq. (4.22) and the renormalized coupling parameters $u[\tau]$, $\gamma[\tau]$, $w[\tau]$, $F[\tau]$, and $f[\tau]$ were determined as functions of τ in Ref. 13. We identify $\mu l = \xi^{-1}$ by the correlation length $\xi = \xi(\tau)$, which in the asymptotic region is given by $\xi(\tau) = \xi_0\tau^{-\nu}$. The identification $\mu l = \xi^{-1}$ is correct in one-loop order, corrections appear in higher orders.[30]

Now, we write the self-consistent equations for the effective parameters in a form which is appropriate for the numerical evaluation. For this purpose we eliminate some of the dimensionless parameters and introduce some new parameters. First of all we note that the asymptotic series (3.21) is not useful to evaluate the function $\Phi_\alpha(X)$. In Ref. 3 an integral representation was found by

$$\Phi_\alpha(X) = [\Gamma(\alpha)]^{-1}\zeta^\alpha\mathcal{F}_\alpha(\zeta)$$

(4.27)

where $\zeta = (-X)^{-1/3}$ and

$$\mathcal{F}_\alpha(\zeta) = \int_0^\infty dv\, v^{\alpha-1}\exp(-v^3 - v\zeta).$$

(4.28)

The integral is well defined for $\alpha > 0$. For $\alpha < 0$ the function $\mathcal{F}_\alpha(\zeta)$ is obtained by analytical continuation in α or equivalently by partial integration in Eq. (4.28) to remove the ultraviolet divergence. Now, we introduce the parameter

$$\sigma = -\frac{1}{12}\left[\rho_1'^2 + 2\frac{w''[\tau]}{w'[\tau]}\left(\frac{F[\tau]\Delta\rho'}{4\gamma[\tau]w'[\tau]}\right)\rho_1' \right.$$
$$\left. -\left(\frac{F[\tau]\Delta\rho'}{4\gamma[\tau]w'[\tau]}\right)^2\right] \tag{4.29}$$

so that $X = -\sigma/\rho_1^3$ or equivalently $\rho_1 = \sigma^{1/3}\zeta$. In the following we eliminate ρ_1 and X in favor of ζ and σ. For convenience we define the amplitudes

$$A = \epsilon^{-1}[\Phi_{-1+\epsilon/2}(X)\rho_1^{-\epsilon/2} - 1] \tag{4.30}$$

$$= \frac{1}{\epsilon}\left[\frac{\sigma^{-\epsilon/6}}{\Gamma(-1+\epsilon/2)}\zeta^{-1}\mathcal{F}_{-1+\epsilon/2}(\zeta) - 1\right], \tag{4.31}$$

$$A_1 = \epsilon^{-1}[(1-\epsilon/2)\Phi_{\epsilon/2}(X)\rho_1^{-\epsilon/2} - 1] \tag{4.32}$$

$$= \frac{1}{\epsilon}\left[-\frac{\sigma^{-\epsilon/6}}{\Gamma(-1+\epsilon/2)}\mathcal{F}_{\epsilon/2}(\zeta) - 1\right]. \tag{4.33}$$

Then we rewrite Eq. (4.14) as

$$\rho = \sigma^{1/3}\zeta\{1 + 8u[\tau]A\}. \tag{4.34}$$

To eliminate ρ we insert this into Eq. (4.22). Resolving with respect to the temperature difference we obtain

$$\Delta T(z) = T(z) - T_\lambda(z) = T_\lambda \tau \sigma^{1/3}\zeta\{1 + 8u[\tau]A\}. \tag{4.35}$$

Next we resolve Eq. (4.20) with respect to $\Delta\rho'$ and obtain

$$\Delta\rho' = -\frac{2\gamma[\tau]F[\tau]}{A_d}\left(\frac{Q\xi^{d-1}}{g_0 k_B T_\lambda}\right) \Big/ \{1 + (f[\tau]/2)A_1\}. \tag{4.36}$$

Resolving Eq. (4.15) with respect to ρ_1' and eliminating ρ' by inserting Eq. (4.24) we obtain

$$\rho_1' = \left[\Delta\rho' - \frac{1}{\tau}\frac{\xi}{T_\lambda}\frac{\partial T_\lambda}{\partial z}\right] \Big/ \{1 + 8u[\tau]A_1\}. \tag{4.37}$$

Finally, from Eq. (4.23) we obtain the temperature gradient

$$\partial_z T = T_\lambda(\tau/\xi)\Delta\rho'. \tag{4.38}$$

Until now the RG flow parameter τ is arbitrary. We must choose τ so that an optimum resummation of the infrared divergences in the perturbation series is achieved. From our experience we find that the condition

$$\sigma^{1/3}(8 + \zeta - 16u[\tau]A\zeta) = 1 \tag{4.39}$$

is an optimum choice for fixing the RG flow parameter τ. For $Q \to 0$ in thermal equilibrium Eq. (4.39) reduces to the well-known flow parameter conditions of the previous theories[13] above and below T_λ. The integral (4.28) can be evaluated asymptotically for large positive and negative ζ. For $\zeta \gg +1$ we find

$$\mathcal{F}_\alpha(\zeta) \approx \Gamma(\alpha)\zeta^{-\alpha} \tag{4.40}$$

which implies $\Phi_\alpha(X) \approx 1$. Consequently, from Eqs. (4.30)–(4.33) we obtain the amplitudes

$$A \approx \epsilon^{-1}[\rho_1^{-\epsilon/2} - 1], \tag{4.41}$$

$$A_1 \approx \epsilon^{-1}[(1-\epsilon/2)\rho_1^{-\epsilon/2} - 1]. \tag{4.42}$$

The flow parameter Eq. (4.39) reduces to $\rho_1(1 - 16u[\tau]A) = 1$ which implies

$$r(l)/(\mu l)^2 = \rho = \rho_1 = 1. \tag{4.43}$$

Equation (4.22) implies $T > T_\lambda$ and $\tau = (T - T_\lambda)/T_\lambda$ so that the RG flow parameter τ is identified by the reduced temperature. Indeed, Eq. (4.43) is the flow-parameter equation of the previous theories[13] in thermal equilibrium for $T > T_\lambda$. On the other hand for $\zeta \ll -1$ we find

$$\mathcal{F}_\alpha(\zeta) \approx (\pi/3)^{1/2}(-\zeta/3)^{\alpha/2 - 3/4}\exp\{2(-\zeta/3)^{3/2}\} \tag{4.44}$$

which is exponentially large. Consequently, the amplitudes A and A_1 are exponentially large so that in Eq. (4.34) and in the flow parameter condition (4.39) only the last terms are relevant. Eliminating A we obtain

$$-2r(l)/(\mu l)^2 = -2\rho = 1 \tag{4.45}$$

which is the flow-parameter equation of the previous theories for $T < T_\lambda$. Equation (4.22) implies $\tau = -2(T - T_\lambda)/T_\lambda$ and $T < T_\lambda$. We conclude that our present theory for nonzero Q reduces to the previous theories[13] for $\zeta \gg +1$ in the normal-fluid region well above T_λ and for $\zeta \ll -1$ in the superfluid region well below T_λ.

We have derived seven equations given by Eqs. (4.29), (4.31), (4.33), (4.35)–(4.37), and (4.39) which we have published already for $d = 3$ and $\epsilon = 1$.[19] These equations contain seven variables ζ, σ, τ, A, A_1, $\Delta\rho'$, ρ_1' which can be determined uniquely by solving the equations supposed the temperature difference $\Delta T = T - T_\lambda$ and the heat current Q are known. The remaining effective parameters, which we have eliminated, can be determined afterwards. In practice we have solved the equations for $d = 3$ dimensions and $\epsilon = 1$ in the following way. While the heat current Q is assumed to be constant we take ζ as a variable which we vary in the whole interval $-\infty < \zeta < +\infty$ to scan all temperatures. Equation (4.39) is solved explicitly to obtain σ as a function of ζ and τ. Then we solve the equations numerically by adjusting the flow parameter τ and eventually determine the temperature difference ΔT and the temperature gradient $\partial_z T$ as functions of ζ by Eqs. (4.35) and (4.38).

As an input we need the dimensionless renormalized couplings $u[\tau]$, $\gamma[\tau]$, $w[\tau] = w'[\tau] + iw''[\tau]$, $F[\tau]$, and $f[\tau]$ as functions of τ which have been determined by Dohm.[13] Furthermore, we need the parameter g_0 which is related to the entropy at T_λ. For liquid helium at saturated vapor pressure this parameter is[31] $g_0 = 2.164 \times 10^{11}$ s^{-1}. To calculate the correlation length $\xi(\tau) = \xi_0\tau^{-\nu}$ as a function of τ we use the exponent $\nu = 0.671$ and the amplitude $\xi_0 = 1.45 \times 10^{-8}$ cm which were determined experimentally in Refs. 31 and 32. There are no adjustable parameters.
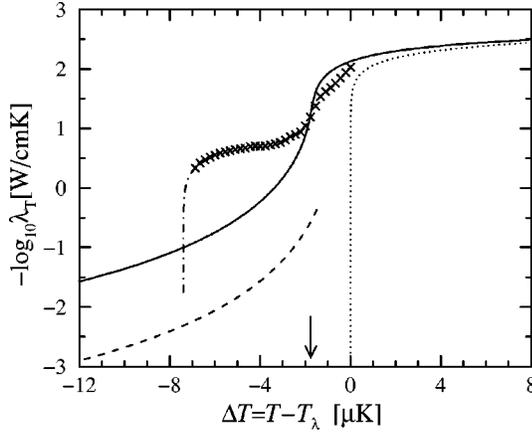
FIG. 3. The thermal resistivity $\rho_T = 1/\lambda_T$ logarithmically as a function of $\Delta T = T - T_\lambda$ for the heat current $Q = 42.9$ μW/cm^2. The solid line represents our theory. The data of Liu and Ahlers[6] are shown as crosses, and the data of Baddar et al.[17] (fit formula) are shown as dashed line. The arrow indicates $\Delta T_\lambda(Q)$. The dash-dotted line extrapolating the crosses indicates $\Delta T_c(Q)$. For comparison, the thermal resistivity for $Q = 0$ (theory) is shown as dotted line.

V. THERMAL CONDUCTIVITY

A. Numerical evaluation of the thermal conductivity and comparison with experiments

We eliminate $\Delta \rho'$ from Eqs. (4.36) and (4.38) and re-solve the resulting equation with respect to Q. Then we obtain the heat transport equation

$$Q = -\lambda_T \partial_z T, \qquad (5.1)$$

where

$$\lambda_T = \frac{g_0 k_B A_d}{\tau \xi^{d-2}} \frac{\{1 + (f[\tau]/2)A_1\}}{2\gamma[\tau]F[\tau]} \qquad (5.2)$$

is the thermal conductivity. Inserting the dimensionless parameters into Eq. (5.2), which we calculate for given ΔT and Q as described above by solving the seven equations, we obtain the thermal conductivity $\lambda_T = \lambda_T(\Delta T, Q)$ as a function of ΔT and Q. The result is obtained without adjustable parameters. We plot the thermal resistivity $\rho_T = 1/\lambda_T$ logarithmically as a function of $\Delta T = T - T_\lambda$ for given heat currents Q. In Fig. 3 our result is shown for $Q = 42.9$ μW/cm^2 as solid line. First of all we find that ρ_T is nonzero and λ_T is finite for all temperatures above and below T_λ. For T well above T_λ and well below T_λ we approximately find asymptotic power laws, which we will discuss in the next subsection.

In the intermediate region, where T is close to T_λ, the curve interpolates the two approximate power laws and shows a point of maximum slope. We may interpret this point as the superfluid transition and define the related shift of the critical temperature $\Delta T_\lambda(Q)$, which in Fig. 3 is indicated by the arrow. In the previous theory[4] the formula

$$\Delta T_\lambda(Q) = -M T_\lambda \left(\frac{Q\xi_0^{d-1}}{g_0 k_B T_\lambda} \right)^x \qquad (5.3)$$

was derived for the shift of the critical temperature with the exponent $x = [(d-1)\nu]^{-1} = 0.745$ and the constant $M = 2.90$ for $d = 3$ dimensions. Here we use Eq. (5.3) as a fit formula for the point of maximum slope in Fig. 3. By varying the heat current Q we find nearly the same exponent $x = 0.745$ where deviations due to nonasymptotic effects of the dynamic RG theory are very small here. Furthermore, we find the constant $M = 3.17$ which also is nearly the same. Thus the point of maximum slope in Fig. 3 may indeed be identified as the superfluid transition. However, in contrast to the previous theory,[4] here $\Delta T_\lambda(Q)$ and the superfluid transition are not sharply defined for nonzero Q because the curves of the physical quantities are smooth.

For zero heat current (linear response limit) the thermal conductivity is shown as dotted line in Fig. 3, which is finite for $\Delta T > 0$, diverges at $\Delta T = 0$, and is infinite for $\Delta T < 0$. Clearly, the solid line of our present theory [$\lambda_T(\Delta T, Q)$ at nonzero Q] approaches the dotted line (λ_T at $Q = 0$) asymptotically in the normal-fluid region for large positive ΔT. Furthermore, the present theory reproduces the previous theory of Ref. 3 for $\Delta T \gtrsim 0$. Some small deviations of the two approaches from each other occur because here and in Ref. 3 the RG flow parameter τ is determined by different conditions [the condition (4.39) here differs from Eq. (4.49) in the second paper of Ref. 3]. However, these deviations are within the errors of the RG theory and hence are not serious.

Liu and Ahlers[6] considered a vertical heat flow upwards in liquid ^{4}He. They measured the temperatures at the bottom and at the top of the cell and determined the thermal conductivity $\lambda_T(\Delta T, Q)$ in two different ways. First, they used a fit formula with power laws for $\lambda_T(\Delta T, Q)$ and adjusted the exponents and amplitudes. Second, they obtained λ_T by the differential formula (24) of the first paper of Ref. 3. In Fig. 3 the data obtained by the differential formula are shown as crosses. For lower temperatures the data are extrapolated by the fit formula shown as dash-dotted line. While $\Delta T_\lambda(Q)$ is indicated by the arrow, the data show the second transition temperature $\Delta T_c(Q)$ where the dash-dotted line drops down nearly vertically. In the normal-fluid region for $\Delta T \gtrsim \Delta T_\lambda(Q)$ the experimental data agree with our theoretical prediction (solid line) within the accuracies of theory and experiment. However, in the superfluid region for $\Delta T \lesssim \Delta T_\lambda(Q)$ the data of Liu and Ahlers[6] do not agree with our theory. For temperatures ΔT in the interval $\Delta T_c(Q) \lesssim \Delta T \lesssim \Delta T_\lambda(Q)$, the so-called dissipative region,[6] the experiment finds a much larger thermal resistivity $\rho_T = 1/\lambda_T$, by about a factor of 20, than our theory predicts. Then suddenly, when the temperature ΔT approaches and drops below the second transition temperature $\Delta T_c(Q)$, the experimentally observed thermal resistivity is so small, that it was not detected any more in the experiment.[6] Our theory does not predict the second transition temperature $\Delta T_c(Q)$, which has been found in the experiments.[5,6,8] While the solid line in Fig. 3 has an inflection point with maximum slope at $\Delta T_\lambda(Q)$, nothing unusual is found at $\Delta T_c(Q)$.

The experiments of Refs. 6 and 8 were performed by measuring the temperatures at the bottom plate and at the top plate, where the heat current flows into and out of the helium. For this reason, these experiments may be influenced considerably by surface effects. In superfluid ^{4}He the dissipation of the heat current is caused by creation of vortices,

where the thermal resistivity $\rho_T = 1/\lambda_T$ is proportional to the density of vortices in the helium. Near the bottom and top surfaces additional vortices may be created which enhance the vortex density there. This effect may possibly explain the strong enhancement of the experimentally observed[6] thermal resistivity for temperatures ΔT in the interval $\Delta T_c(Q) \lesssim \Delta T \lesssim \Delta T_\lambda(Q)$ (see crosses in Fig. 3).

In a recent experiment Baddar *et al.*[17] measured the temperature gradient $\partial_z T$ in superfluid helium for several heat currents Q. To exclude surface effects at the bottom and top plates the temperatures were measured by sidewall thermometers only. The thermal conductivity $\lambda_T(\Delta T, Q)$ was then obtained from the heat transport equation (5.1). A power-law fit formula for $\lambda_T(\Delta T, Q)$ was found which is valid for a wide range of heat currents Q and temperatures ΔT sufficiently below $\Delta T_\lambda(Q)$. In Fig. 3 the thermal resistivity $\rho_T = 1/\lambda_T$ for $Q = 42.9$ μW/cm^2 represented by this fit formula is shown as dashed line. Clearly, the temperature dependence of the experimental data agrees qualitatively with the theoretical prediction (solid line). However, the absolute values of the measured thermal resistivity are about a factor of 20 smaller than the theoretically predicted values. While the experiment of Baddar *et al.*[17] is believed to be a better and more direct measurement of the thermal conductivity or resistivity, there remains a disagreement between experiment and theory.

We may possibly explain the discrepancy in the following way. In superfluid ^{4}He a homogeneous heat current Q represents a metastable state.[4] For the creation of vortices energy barriers must be overcome. This fact keeps the rate of vortex creation low so that the vortex density and hence the thermal resistivity are small. On the other hand, our theory is based on the approximation where the complex order parameter ψ is replaced by a vector $\Psi = (\psi_1, \ldots, \psi_n)$ of n complex components in the limit $n \to \infty$. In this limit the heat current Q is always unstable so that the rate of vortex creation is higher. Consequently, in our theory the vortex density and hence the thermal resistivity are expected to be larger. However, the large discrepancies in Fig. 3 indicate that the vortex density is a very sensitive quantity which may be influenced strongly by the kind of the approximation in theory and by certain conditions in the experiment.

B. Asymptotic formulas for the thermal conductivity

For temperatures T well above T_λ Eqs. (4.41)–(4.43) imply $A = 0$ and $A_1 = -1/2$ so that λ_T depends only on $\tau = \Delta T/T_\lambda$ but not on the heat current. Thus well above T_λ the heat transport described by Eq. (5.1) is linear. From Eq. (5.2) we recover the well-known result of Ref. 13 for λ_T at infinitesimal Q in one-loop order. Asymptotically in leading order we find

$$\lambda_T \sim \tau^{-1} \xi^{-(d-2)} \sim \Delta T^{-1+(d-2)\nu} \qquad (5.4)$$

which diverges in the limit $\Delta T \to 0$. For $d = 3$ including nonasymptotic effects of the dynamic RG theory one obtains $\lambda_T \sim \Delta T^{-0.44}$. Thus near T_λ the thermal conductivity is strongly enhanced by critical fluctuations.

However, at fixed nonzero Q for temperatures T close to T_λ the flow parameter τ will reach a minimum value and the correlation length ξ will reach a maximum value, so that λ_T

remains finite even at T_λ. This fact was found previously in Ref. 3 and is seen clearly in Fig. 3. The thermal conductivity $\lambda_T = \lambda_T(\Delta T, Q)$ becomes Q dependent so that the heat transport is nonlinear. The crossover from linear to nonlinear heat transport happens for temperatures ΔT below[3]

$$\Delta T_{nl}(Q) = M_{nl} T_\lambda \left(\frac{Q\xi_0^{d-1}}{g_0 k_B T_\lambda} \right)^x \qquad (5.5)$$

with the exponent $x = [(d-1)\nu]^{-1}$, where M_{nl} is a constant of order unity. For $d = 3$ the values $x = 0.745$ and $M_{nl} \approx 2.8$ were found.[3]

While the previous theory[3] is valid only for $\Delta T \gtrsim 0$, the present theory works also for lower temperatures in the superfluid region. Well below T_λ the thermal conductivity (5.2) can be evaluated asymptotically. For $\zeta \lesssim -5$ the function $\mathcal{F}_\alpha(\zeta)$ approximated by Eq. (4.44) is exponentially large. Consequently, the amplitudes A and A_1 are exponentially large. From Eqs. (4.31) and (4.33) we obtain the ratio

$$\frac{A_1}{A} \approx -\frac{\zeta \mathcal{F}_{\epsilon/2}(\zeta)}{\mathcal{F}_{-1+\epsilon/2}(\zeta)} \approx 3^{-1/2}(-\zeta)^{3/2}. \qquad (5.6)$$

Equations (4.36) and (4.37) reduce to

$$\frac{F[\tau]\Delta\rho'}{4\gamma[\tau]w'[\tau]} \approx -\frac{1}{A_d}\left(\frac{Q\xi^{d-1}}{g_0 k_B T_\lambda} \right) \frac{1}{A_1}, \qquad (5.7)$$

$$\rho_1' \approx -\frac{1}{\tau}\frac{\xi}{T_\lambda}\frac{\partial T_\lambda}{\partial z}\frac{1}{8u[\tau]}\frac{1}{A_1}. \qquad (5.8)$$

We assume that the heat current Q is sufficiently large so that gravity effects may be neglected and Eq. (5.8) is much smaller than Eq. (5.7). Then, from Eq. (4.29) we obtain

$$\sigma \approx \frac{1}{12 A_d^2}\left(\frac{Q\xi^{d-1}}{g_0 k_B T_\lambda} \right)^2 \frac{1}{A_1^2}. \qquad (5.9)$$

On the other hand, the flow parameter equation (4.39) reduces to

$$\sigma^{1/3} 16 u[\tau] A(-\zeta) = 1. \qquad (5.10)$$

Now, Eqs. (5.6), (5.9), and (5.10) are three equations for A, A_1, and σ. Eliminating σ we obtain the amplitudes

$$A \approx \frac{1}{2}\frac{A_d^2}{(8u[\tau])^3}\left(\frac{g_0 k_B T_\lambda}{Q\xi^{d-1}} \right)^2, \qquad (5.11)$$

$$A_1 \approx \frac{(-\zeta)^{3/2}}{2\sqrt{3}}\frac{A_d^2}{(8u[\tau])^3}\left(\frac{g_0 k_B T_\lambda}{Q\xi^{d-1}} \right)^2. \qquad (5.12)$$

Eventually, from Eq. (5.2) we obtain the thermal conductivity

$$\lambda_T \approx \frac{g_0 k_B}{\tau\xi^{d-2}}\frac{F[\tau]}{4\gamma[\tau]w'[\tau]}\frac{1}{\sqrt{12}}\left(\frac{(-\zeta)^{1/2}A_d}{8u[\tau]} \right)^3 \left(\frac{g_0 k_B T_\lambda}{Q\xi^{d-1}} \right)^2, \qquad (5.13)$$

where $\tau = -2\Delta T/T_\lambda$. The variable ζ depends only weakly on τ, i.e., logarithmically. Thus asymptotically in leading order we find

$$\lambda_T \sim \tau^{-1}\xi^{4-3d}Q^{-2} \sim (-\Delta T)^{(3d-4)\nu-1}Q^{-2}. \quad (5.14)$$

For $d=3$ including nonasymptotic effects we obtain $\lambda_T \sim (-\Delta T)^{2.4}Q^{-2}$.

In their experiment Baddar et al.[17] have found that for a wide range of heat currents Q the thermal conductivity can be expressed in terms of the power-law formula

$$\lambda_{T,exp} = \lambda_0[(-\Delta T/T_\lambda)(Q/Q_0)^{-0.904}]^{2.8} \quad (5.15)$$

$$\sim (-\Delta T)^{2.8}Q^{-2.53}, \quad (5.16)$$

where $\lambda_0 = 1$ W/cm K and $Q_0 = 393$ W/cm^2. Clearly, this power-law formula has the same structure as the asymptotic formula (5.14) of our theoretical prediction. However, the two formulas do not agree quantitatively with each other. The exponents of the power laws differ by about 20%. Furthermore, the amplitudes differ by a factor of 20 which means that $\lambda_{T,exp}$ is about 20 times larger than the theoretical λ_T (see dashed and solid line in Fig. 3). The discrepancies may possibly be due to the approximation we have used in our theory. Further theoretical and experimental work is necessary to clarify the origin of the discrepancies.

C. Influence of gravity

On earth gravity implies a spatially dependent superfluid transition temperature $T_\lambda(z)$ with a nonzero gradient $\partial_z T_\lambda = \pm 1.273$ μK/cm. Supposed the heat current Q is flowing in the z direction the gradient $\partial_z T_\lambda$ is positive for heat current upwards and negative for heat current downwards. In our theory the gradient $\partial_z T_\lambda$ is incorporated in Eq. (4.24) or equivalently in Eq. (4.37). We find that on earth the effects of heat current Q and of gravity have equal magnitude for $Q \approx 65$ nW/cm^2. For larger Q the heat current is dominating while for smaller Q gravity is dominating. We find that for $Q \gtrsim 1$ μW/cm^2 the effects of gravity are very small so that in this case gravity can be neglected. The experiments by Liu and Ahlers,[6] Murphy and Meyer,[8] and the experiment by Baddar et al.[17] are performed at heat currents Q which satisfy this condition.

We have performed our calculations for a positive and a negative gradient $\partial_z T_\lambda$ representing gravity on earth and also for a zero gradient $\partial_z T_\lambda$ which corresponds to a microgravity environment in space. As a result, for heat currents $Q \gtrsim 100$ nW/cm^2 the thermal conductivity $\lambda_T(\Delta T, Q)$ is nearly independent of gravity. On the other hand, for heat currents $Q \lesssim 80$ nW/cm^2 our theory fails if gravity is present, because σ defined in Eq. (4.29) changes sign so that no solution of the seven equations for the dimensionless parameters in Sec. IV can be found.

Day et al.[33] investigated the superfluid–normal-fluid interface in ^{4}He and measured the thermal conductivity λ_T for very small heat currents Q in the interval 20 nW/cm$^2 < Q < 6$ μW/cm^2. The heat current flows upwards so that the gradient $\partial_z T_\lambda$ is positive. Clearly, this experiment explores the crossover from the gravity dominated region to the heat current dominated region. For heat currents Q

$\gtrsim 100$ nW/cm^2 the experimental data agree quite well with our theoretical prediction for λ_T. This has been demonstrated in our previous rapid communication[19] for temperatures $\Delta T \gtrsim \Delta T_\lambda(Q)$ (see Fig. 2 therein). In the superfluid region for $\Delta T \lesssim \Delta T_\lambda(Q)$ the thermal resistivity is very small so that here experimental data are not available with sufficient accuracy on a logarithmic scale.

For very low heat currents $Q \lesssim 40$ nW/cm^2 the data of Day et al.[33] indicate that the thermal resistivity $\rho_T = 1/\lambda_T(\Delta T, Q)$ is a smooth function of ΔT in the limit $Q \to 0$ if gravity is present. This fact means that gravity prevents the system from reaching the critical point of the superfluid transition, so that all physical quantities are smooth and nonsingular near T_λ. Unfortunately, our theory fails for these low heat currents in the gravity dominated region. However, an alternative approach is possible which is equivalent to Onuki's theory.[2] In mean-field approximation the model-F equations (2.1) and (2.2) can be solved numerically as partial differential equations to obtain the order-parameter profile and the temperature profile of the superfluid–normal-fluid interface. To include the critical fluctuations the model-F equations are renormalized and the RG theory is applied. The approach is a renormalized mean-field theory which works for all heat currents Q and gravity, even for very small Q in the gravity dominated region. In this way we obtain a thermal resistivity $\rho_T = 1/\lambda_T(\Delta T, Q)$ which agrees qualitatively with the experimental observation of Day et al.:[33] it is a smooth function of ΔT and nearly independent of Q for $Q \lesssim 10$ nW/cm^2 including the limit $Q \to 0$. In agreement with the experiment[33] we find that $\delta T_g \approx 15$ nK is the relevant temperature scale on which the critical singularity is smoothened by gravity. This temperature scale is related to the thickness of the superfluid–normal-fluid interface $\xi_g \approx 100$ μm by $\delta T_g/\xi_g \approx |\partial_z T_\lambda| = 1.273$ μK/cm.

To measure the critical singularity of the thermal resistivity or conductivity for heat currents smaller than 100 nW/cm^2 and temperatures closer than 15 nK to the superfluid transition, the experiment must be performed under microgravity conditions in space. Of course, for zero gravity where $\partial_z T_\lambda = 0$ our theory presented in this paper works for all heat currents and never fails at any low Q.

VI. TEMPERATURE PROFILE

A. Numerical results

Once the thermal conductivity $\lambda_T = \lambda_T(\Delta T, Q)$ has been determined, the temperature profile $T(z)$ is calculated by solving the heat transport equation (5.1) as a differential equation which can be written in the form

$$\frac{\partial T}{\partial z} = -\frac{Q}{\lambda_T(\Delta T, Q)}, \quad (6.1)$$

where $\Delta T = T(z) - T_\lambda(z)$. In Fig. 4 the resulting temperature profile of the superfluid–normal-fluid interface is shown for $Q=1$ μW/cm^2. The several curves correspond to all three gravity conditions as indicated in the figure: vertical heat flow *upwards* and vertical heat flow *downwards* on earth and heat flow in *zero gravity* in space. The temperature profiles $T(z)$ are shown as solid lines. The spatially dependent critical temperatures $T_\lambda(z)$, which represent the gravity condi-
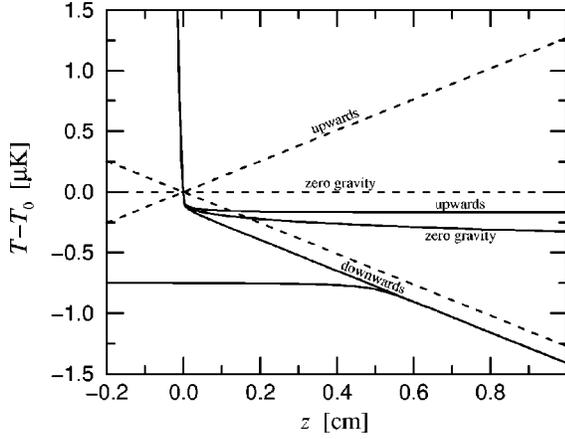
FIG. 4. The temperature profile of the superfluid–normal-fluid interface for the heat current $Q = 1$ μW/cm^2 for the three gravity conditions: vertical heat flow *upwards* and *downwards* on earth and heat flow in *zero gravity* in space. While the solid lines correspond to the temperature profiles $T(z)$, the dashed lines represent the spatially dependent critical temperatures $T_\lambda(z)$, which reflect the gravity conditions.

tions, are shown as dashed lines. While in Sec. V we have found that $\lambda_T(\Delta T, Q)$ does not depend on gravity for $Q \gtrsim 0.1$ μW/cm^2, the temperature profile $T(z)$ is considerably influenced by gravity which is clearly seen in Fig. 4 because there are several solid lines.

In Fig. 4 we have chosen the coordinates so that the superfluid–normal-fluid interface, where $\Delta T = T(z) - T_\lambda(z)$ $= 0$, is located at $z = 0$ and $T(z) = T_0$. For this reason all curves intersect with each other in the point (0,0). For $z < 0$ the helium is normal fluid because $\Delta T = T(z) - T_\lambda(z)$ > 0 so that the solid line is above the respective dashed line. On the other hand for $z > 0$ the helium is superfluid because here $\Delta T = T(z) - T_\lambda(z) < 0$ so that the respective solid line is below the respective dashed line. (Since the many curves in Fig. 4 may be confusing, one should have in mind that only those solid and dashed lines should be compared with each other which belong to the same gravity condition.) Furthermore, we have chosen a strongly enlarged temperature scale (in μK) which resolves the very small temperature gradients in the superfluid region $z > 0$. For this reason in the normal-fluid region $z < 0$ the solid line in Fig. 4 [temperature profile $T(z)$] has a very steep gradient and goes up nearly vertically for decreasing z. The shifted critical temperature $\Delta T_\lambda(Q)$, which here is -0.10 μK, is located approximately at this point where the solid line has a ''round corner'' and the gradient changes from large negative to small negative.

In the normal-fluid region $z \lesssim 0$ where $\Delta T \gtrsim \Delta T_\lambda(Q)$ the three solid lines fall all together into one line which indicates that here gravity is negligible. On the other hand in the superfluid region $z \gtrsim 0$ where $\Delta T \lesssim \Delta T_\lambda(Q)$ all three solid lines differ from each other which means that here gravity is important. A general criterion can be found to distinguish the regions where gravity is important and where it is negligible. In the differential equation (6.1) gravity is included implicitly via $\Delta T = T(z) - T_\lambda(z)$ by the gradient of the critical temperature $T_\lambda(z)$. Gravity will be important or not if the spatial dependence of $T_\lambda(z)$ or of $T(z)$ is dominating. We may
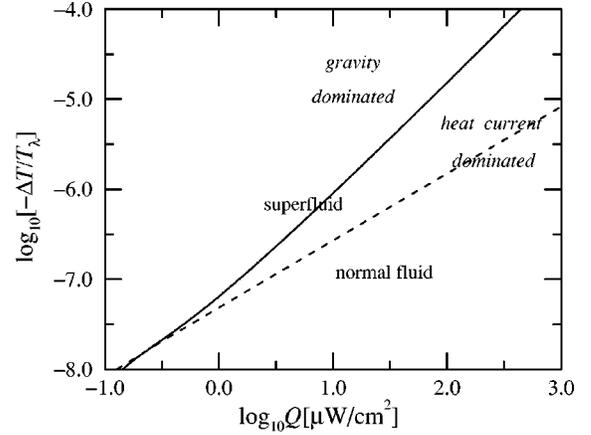

FIG. 5. The temperature shifts $\Delta T_1(Q)$ (solid line) and $\Delta T_\lambda(Q)$ (dashed line), obtained from Eqs. (6.2) and (5.3), respectively, as functions of the heat current Q in a double logarithmic plot. $\Delta T_1(Q)$ separates the gravity dominated region from the heat current dominated region, while $\Delta T_\lambda(Q)$ separates the superfluid region from the normal-fluid region.

define the Q-dependent temperature difference $\Delta T_1(Q)$ by the condition $|\nabla T| = |\nabla T_\lambda|$, which in terms of Eq. (6.1) can be written as

$$\frac{Q}{\lambda_T(\Delta T_1(Q), Q)} = \left| \frac{\partial T_\lambda}{\partial z} \right| = 1.273 \quad \mu\text{K/cm}. \quad (6.2)$$

For $\Delta T > \Delta T_1(Q)$ it is $|\nabla T| > |\nabla T_\lambda|$ so that the heat current is dominating. On the other hand, for $\Delta T < \Delta T_1(Q)$ it is $|\nabla T| < |\nabla T_\lambda|$ so that gravity is dominating. Consequently, for temperatures ΔT sufficiently well above $\Delta T_1(Q)$ it is $|\nabla T| \ll |\nabla T_\lambda|$ so that gravity can be neglected while otherwise gravity effects are significant. Thus $\Delta T_1(Q)$ may be viewed as the temperature which separates the heat current dominated region from the gravity dominated region.

For the heat current $Q = 1$ μW/cm^2 in Fig. 4 we find $\Delta T_1(Q) = -0.14$ μK which is slightly below but close to $\Delta T_\lambda(Q) = -0.10$ μK. Thus in this case the interface between the superfluid and the normal-fluid region nearly coincides with the interface which separates the gravity dominated region from the heat current dominated region. This fact is clearly seen in Fig. 4. For other heat currents Q the situation may change, because $\Delta T_1(Q)$ and $\Delta T_\lambda(Q)$ may be farther apart from each other. In Fig. 5 we plot $\Delta T_1(Q)$ and $\Delta T_\lambda(Q)$ as functions of Q on a double logarithmic scale. Our theoretical result for $\Delta T_1(Q)$ obtained from Eq. (6.2) is shown as solid line. Furthermore, $\Delta T_\lambda(Q)$ obtained from Eq. (5.3) is shown as dashed line. For the heat currents $Q \gtrsim 0.1$ μW/cm^2, for which our theory is valid in gravity, both $\Delta T_\lambda(Q)$ and $\Delta T_1(Q)$ are negative. While in Fig. 5 the solid line represents $\Delta T_1(Q)$ for vertical heat flow downwards, $\Delta T_1(Q)$ for vertical heat flow upwards will be slightly different. However, the difference is very small. It is smaller than the width of the solid line so that it can be neglected. Thus the solid line in Fig. 5 represents $\Delta T_1(Q)$ for both heat flow directions with sufficient accuracy.

For $Q = 0.22$ μW/cm^2, in Fig. 5 the solid line and the dashed line intersect each other so that $\Delta T_1(Q) = \Delta T_\lambda(Q)$. For larger heat currents $\Delta T_1(Q)$ is always below $\Delta T_\lambda(Q)$ so that the separation between the gravity dominated and the heat current dominated region is located always in the superfluid region or equivalently the superfluid–normal-fluid in-

terface is located in the heat current dominated region. It turns out that for sufficiently large heat currents, say $Q \gtrsim 10 \ \mu\mathrm{W/cm^2}$, the superfluid–normal-fluid interface is nearly free from influences of gravity, while gravity effects rise to a significant magnitude only far away from the interface in the superfluid region. However, since the interface thickness must be larger than the size of the thermometers, experiments to resolve the temperature profile of the superfluid–normal-fluid interface must be performed for very small heat currents $Q \lesssim 0.1 \ \mu\mathrm{W/cm^2}$. For these small heat currents, on earth the interface would be strongly influenced by gravity. For this reason, an experiment to measure the temperature profile of the interface is prepared to be performed under microgravity conditions in space.[34]

B. Asymptotic formulas

By using the asymptotic formulas of the thermal conductivity $\lambda_T(\Delta T, Q)$ in Sec. V B, the differential equation (6.1) can be solved explicitly so that asymptotic formulas for the temperature profile $T(z)$ are found in several regions. First of all we consider the heat flow in zero gravity where $T_\lambda(z) = T_\lambda$ is constant. In this case the differential equation (6.1) can be integrated easily by separation of the variables so that

$$z = -\int_{T_\lambda}^{T} Q^{-1} \lambda_T(T' - T_\lambda, Q) \, dT'. \qquad (6.3)$$

In the normal-fluid region for T sufficiently well above T_λ the asymptotic formula (5.4) may be inserted. Consequently, we obtain

$$\Delta T(z) = T(z) - T_\lambda \approx K_+ (-Qz)^{1/[(d-2)\nu]} \qquad (6.4)$$

for $z \ll 0$ with a certain constant K_+. On the other hand, for T sufficiently well below T_λ the asymptotic formula (5.14) may be inserted which implies

$$\Delta T(z) = T(z) - T_\lambda \approx -K_- (Q^3 z)^{1/[(3d-4)\nu]} \qquad (6.5)$$

for $z \gg 0$ with a certain constant K_-. Including the nonasymptotic effects of the dynamic RG theory, for the temperature profile $T(z)$ we obtain the asymptotic formula

$$T(z) \approx \begin{cases} T_\lambda + K_+ (-Qz)^{1.79} & \text{for } z \ll 0 \\ T_\lambda - K_- (Q^3 z)^{0.294} & \text{for } z \gg 0 \end{cases} \qquad (6.6)$$

which is valid for the heat flow in zero gravity. This formula can be compared with the solid line in Fig. 4 for zero gravity. Clearly, the temperature profile $T(z)$ decreases monotonically with increasing z. There is no lower bound for $T(z)$ in the limit $z \to \infty$.

Asymptotic formulas for the temperature profile $T(z)$ can be found also for vertical heat flows in gravity. The interface, which separates the heat current dominated region from the gravity dominated region, is located at a coordinate z_1 defined by $\Delta T(z_1) = \Delta T_1(Q)$. For $Q > 0.22 \ \mu\mathrm{W/cm^2}$ it is $z_1 > 0$ so that the interface is located in the superfluid region. For $z \ll z_1$ gravity is negligible. Consequently, the asymptotic formula (6.6) remains valid for $z \ll z_1$ where $T_\lambda = T_\lambda(z=0)$ should be inserted. In the case of a vertical heat flow *upwards* another asymptotic formula can be found for $z \gg z_1$. In

Fig. 4 it is clearly seen that in this case the temperature profile approaches a limiting value

$$\lim_{z \to +\infty} T(z) = T_\infty(Q) \qquad (6.7)$$

which is below $T_\lambda(z=0)$. For $z \gg z_1$ the temperature difference is approximately $\Delta T(z) \approx T_\infty(Q) - T_\lambda(z)$ so that its z dependence is governed by $T_\lambda(z)$, i.e., by gravity. Then, by using the asymptotic formula $\lambda_T \sim (-\Delta T)^{2.4} Q^{-2}$ for the thermal conductivity we obtain the asymptotic formula

$$T(z) \approx T_\infty(Q) + K_\infty Q^3 (z - z_0)^{-1.4} \quad \text{for } z \gg z_1, \qquad (6.8)$$

where $K_\infty > 0$ and $z_0 < 0$ are certain constants and $T_\infty(Q) = T_\lambda(z=0) + z_0 \partial_z T_\lambda$.

On the other hand, for a vertical heat flow *downwards* the solid line in Fig. 4 approaches a straight line parallel to the dashed line for $z \gg z_1$ so that the gradients $\partial_z T$ and $\partial_z T_\lambda$ are nearly equal. The distance from criticality $\Delta T(z) = T(z) - T_\lambda(z)$ approaches a constant value given by

$$\lim_{z \to +\infty} \Delta T(z) = \Delta T_1(Q). \qquad (6.9)$$

Consequently, for the temperature profile we find the asymptotic formula

$$T(z) \approx T_\lambda(z) + \Delta T_1(Q) \quad \text{for } z \gg z_1. \qquad (6.10)$$

C. Dissipative region

For the vertical heat flow upwards the asymptotic formulas (6.6) and (6.8) indicate the existence of a dissipative region which may be related to the dissipative region observed in the experiments by Liu and Ahlers[6] and by Murphy and Meyer.[8] The superfluid transition happens in two steps at $z = 0$ and $z = z_1$ or equivalently at the temperatures $\Delta T = \Delta T_\lambda(Q)$ and $\Delta T = \Delta T_1(Q)$. The region $0 \lesssim z \lesssim z_1$, which corresponds to $\Delta T_1(Q) \lesssim \Delta T \lesssim \Delta T_\lambda(Q)$ (in Fig. 5 the region between the solid and the dashed line), may be identified as the dissipative region, because here the temperature profile $T(z)$ has a finite gradient. On the other hand, the region $z \gtrsim z_1$ which corresponds to $\Delta T \lesssim \Delta T_1(Q)$ (in Fig. 5 the region above the solid line) is the really superfluid region, because here the asymptotic formula (6.8) implies a nearly flat temperature profile with a nearly zero gradient. Thus $\Delta T_1(Q)$ may be interpreted as the transition temperature between the dissipative region and the really superfluid region, which should be related to the temperature shift

$$\Delta T_c(Q) = T_\infty(Q) - T_\lambda(z=0) \qquad (6.11)$$

measured in the experiments.[5,6,8] We find that $\Delta T_c(Q)$ obtained from our theory is close to $\Delta T_1(Q)$ and located slightly above the solid line in Fig. 5. From the slopes of the lines in the double-logarithmic plot we obtain effective power laws $\Delta T_1(Q) \sim -Q^x$ and $\Delta T_c(Q) \sim -Q^x$ with nearly the same exponent x, which varies between $x \approx 0.9$ for $0.1 \ \mu\mathrm{W/cm^2} \lesssim Q \lesssim 1 \ \mu\mathrm{W/cm^2}$ and $x \approx 1.25$ for $Q \gtrsim 10 \ \mu\mathrm{W/cm^2}$.

While our theoretical predictions for the dissipative region agree qualitatively with the experimental observations,[5,6,8] there are three major quantitative disagree-

ments. First of all, the experimentally observed dissipation is much larger than the theoretically predicted, because for $\Delta T_c(Q) < \Delta T < \Delta T_\lambda(Q)$ the measured thermal resistivity $\rho_T = 1/\lambda_T$ of Ref. 6 (crosses in Fig. 3) is much larger than the theoretically predicted (solid line in Fig. 3). Second, the experimental $\Delta T_c(Q) \sim -Q^x$ does not agree with the theoretically predicted because the exponent $x_{exp} = 0.81$ of Duncan, Ahlers, and Steinberg[5] is considerably smaller than the theoretical exponent $x \gtrsim 0.9$. Furthermore, our theory predicts a much larger spatial extent $\Delta z = z_1$ of the dissipative region than it is in the experiments[5,6]. We find $\Delta z \gtrsim 0.25$ cm for $Q \gtrsim 10$ μW/cm² which is about the sample size, while the experiments find a spatial extent Δz much smaller than the sample size.

The disagreements may possibly be due to the experiments of Refs. 5, 6, and 8, because in the experiment by Baddar *et al.*[17] the dissipative region has not been observed in this form. We may use the experimental fit formula[17] (5.15) for the thermal conductivity to calculate the related $\Delta T_{1,exp}(Q)$ and $\Delta T_{c,exp}(Q)$ by Eqs. (6.2) and (6.11), respectively. As results we obtain power laws $\sim -Q^x$ with the exponent $x_{exp} = 1.26$. This exponent agrees quite well with our theoretical value $x = 1.25$ for large heat currents. If we plot $\Delta T_{c,exp}(Q)$ in Fig. 5, the respective line would be parallel to the solid line for $Q \gtrsim 10$ μW/cm² but located somewhat below the solid line. Thus there remains a quantitative disagreement which is related to the quantitative disagreement of λ_T. However, $\Delta T_{c,exp}(Q)$ does also not agree with the $\Delta T_c(Q)$ of the previous experiments.[5,6] Thus for the clarification of the disagreements also further experimental work is necessary.

Since the thermal conductivity $\lambda_T(\Delta T, Q)$ (solid line in Fig. 3) is smooth and does not show any unusual behavior at $\Delta T_1(Q)$ and $\Delta T_c(Q)$, these temperatures are not properties of the helium. Rather, $\Delta T_1(Q)$ and $\Delta T_c(Q)$ are implied by gravity and occur when integrating the heat transport equations (5.1) or (6.1) to calculate the temperature profile. Thus we predict that in the experiment in space,[34] where gravity is zero, the $\Delta T_c(Q)$ of the experiments of Refs. 5, 6, and 8 should not be observable and not be existent, while the $\Delta T_\lambda(Q)$ is expected to be found.

D. Self-organized critical state

In gravity for vertical heat flows downwards the gradients $\partial_z T$ and $\partial_z T_\lambda$ are both negative. A situation may arise where both gradients are equal, $\partial_z T = \partial_z T_\lambda$, so that $\Delta T(z) = \Delta T_1(Q)$ is constant over a larger region in space. This state of the helium represents a self-organized critical (SOC) state which was considered theoretically by Onuki[35] and proposed for an experiment by Ahlers and Liu.[36] Recently, Moeur *et al.*[7] have realized the SOC state and measured the distance from criticality $\Delta T(z) = \Delta T_1(Q)$ as a function of the heat current Q for 40 nW/cm² $< Q < 6$ μW/cm². The experimental result agrees quite well with our theoretical prediction for $\Delta T_1(Q)$, while our theory does not include any unknown adjustable parameters. This has been demonstrated in our previous paper[19] for heat currents below 1.5 μW/cm² (see Fig. 3 therein). However, for $Q \gtrsim 1.5$ μW/cm² deviations occur: for a given distance from criticality $\Delta T = \Delta T_1(Q)$ the related heat current Q is larger

in the experiment than in our theory. This fact means that for $Q \gtrsim 1.5$ μW/cm² the dissipation observed in the experiment[7] is smaller than the dissipation predicted by our theory.

The SOC state is stable in the following sense: the distance from criticality $\Delta T(z)$ always converges to the constant value $\Delta T_1(Q)$ for large z according to Eq. (6.9). This fact is clearly seen in Fig. 4. However, there are two possibilities: $\Delta T(z)$ may converge to $\Delta T_1(Q)$ either from *above* or from *below*. In the first case an interface between normal-fluid helium and the SOC state is found, while in the second case an interface between superfluid helium and the SOC state is found. In Fig. 4 the temperature profiles $T(z)$ are shown for both cases, where the superfluid-SOC interface is represented by the lowest solid line. Both kinds of interfaces were realized in the experiment by Moeur *et al.*[7]

Since $\Delta T(z) = \Delta T_1(Q)$ is constant, the SOC state is homogeneous in space so that it is an ideal system for theoretical and experimental investigations. In the Appendix we evaluate the Green's function $G(\mathbf{r}, \mathbf{r}')$ and the related quantities n_s and J_s by assuming r_1 and Δr to be linear functions of the space coordinate $\mathbf{r}$ given by Eqs. (A12) and (A13). While in general this assumption implies an approximation, for the SOC state the assumption is *exactly* satisfied, because r_1 and Δr are directly related to the temperature profiles $\Delta T = T(z) - T_\lambda(z)$ and $T_\lambda(z)$ which are constant and linear in z, respectively.

VII. CORRELATION LENGTHS

The RG theory includes a characteristic length defined by $\xi = (\mu l)^{-1}$, which is called the correlation length. Near criticality our theory yields the asymptotic result $\xi = \xi_0 \tau^{-\nu}$ where[31,32] $\nu = 0.671$ and $\xi_0 = 1.45 \times 10^{-8}$ cm. The correlation length depends on ΔT and Q indirectly via the RG flow parameter $\tau = \tau(\Delta T, Q)$ determined in Sec. IV. In Fig. 6 the correlation length ξ is shown logarithmically as a function of ΔT for $Q = 42.9$ μW/cm², i.e., the same heat current as in Fig. 3. Clearly, ξ increases when ΔT approaches the super-
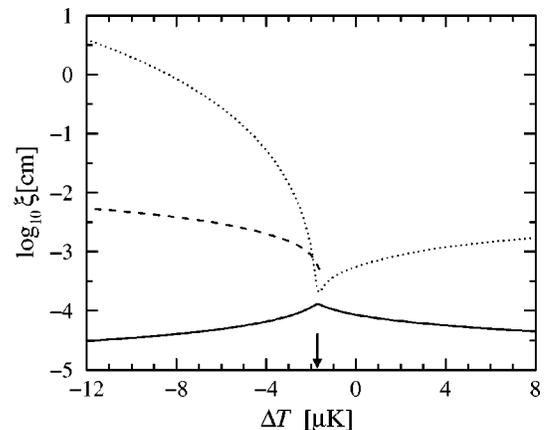

FIG. 6. The correlation lengths as functions of ΔT for the heat current $Q = 42.9$ μW/cm². The correlation length ξ is shown as solid line. The dephasing length ξ_1 obtained from Eq. (7.7) is shown as dashed line. The dotted line represents the characteristic length scale ξ_2 of the temperature variations defined by Eq. (7.11). The arrow indicates $\Delta T_\lambda(Q)$.

fluid transition. The nonzero heat current implies that ξ is a smooth function of ΔT which has a maximum located at $\Delta T_\lambda(Q)$. In Fig. 6 the maximum is clearly shown by the solid line, where its position at $\Delta T_\lambda(Q)$ is indicated by the arrow.

Correlation lengths can be observed in the equal-time Green's function $G(\mathbf{r}, \mathbf{r}')$ because they represent the characteristic length scales for the decay of the Green's function, when the separation of the two space points $|\mathbf{r} - \mathbf{r}'|$ increases. In the normal-fluid region for $\Delta T > \Delta T_\lambda(Q)$ we find

$$G(\mathbf{r}, \mathbf{r}') \rightarrow 0 \quad \text{for} \quad |\mathbf{r} - \mathbf{r}'| \gg \xi \qquad (7.1)$$

which is valid for zero and nonzero heat currents Q. In the superfluid region for $\Delta T < \Delta T_\lambda(Q)$ the decay happens in two steps according to

$$G(\mathbf{r}, \mathbf{r}') \rightarrow \begin{cases} \eta^2 e^{i\mathbf{k}(\mathbf{r} - \mathbf{r}')} & \text{for} \quad \xi \ll |\mathbf{r} - \mathbf{r}'| \ll \xi_1 \\ 0 & \text{for} \quad |\mathbf{r} - \mathbf{r}'| \gg \xi_1 \end{cases}, \qquad (7.2)$$

where ξ_1 is a second correlation length which will be defined below. In this case the decay is strongly influenced by the heat current via $\mathbf{k}$ and ξ_1. In thermal equilibrium where $\mathbf{Q} = \mathbf{0}$ and $\mathbf{k} = \mathbf{0}$, the long-range order implies a nonzero order parameter $\langle \psi \rangle = \eta$ so that ξ_1 is infinite and $G(\mathbf{r}, \mathbf{r}')$ does not decay to zero but only to the absolute square of the order parameter η^2. In the previous theory of Ref. 4 the heat flow is assumed to be metastable where dissipation by creation of vortices was neglected. Thus in this theory long-range order is preserved also for nonzero Q so that $\langle \psi(\mathbf{r}) \rangle = \eta e^{i\mathbf{k}\mathbf{r}}$ is again nonzero, ξ_1 is infinite, and the Green's function does not decay to zero.

However, in the present theory vortices are included implicitly so that $\langle \psi(\mathbf{r}) \rangle = 0$, ξ_1 is finite, and $G(\mathbf{r}, \mathbf{r}')$ decays to zero eventually for large distances. The second correlation length ξ_1 represents a *dephasing length* of the order-parameter field $\psi(\mathbf{r})$ which is equal to the average distance between the vortices. An approximate formula for ξ_1 can be extracted from the integral representation (A28) of the Green's function in the Appendix. In the superfluid region for ΔT sufficiently below $\Delta T_\lambda(Q)$ the exponential factor $\exp\{-\alpha \bar{r}_1 - \alpha^3 s\}$ as a function of α has a sharp maximum located at

$$\alpha_0 = (-\zeta)^{3/2} / [3^{1/2}(-\bar{r}_1)], \qquad (7.3)$$

where $\bar{r}_1$ and $\zeta = s^{-1/3}\bar{r}_1$ are negative. Thus in the second line of Eq. (A28) we may replace α approximately by α_0 so that the integral can be evaluated by Eq. (A29). As a result we obtain the Green's function

$$G(\mathbf{r}, \mathbf{r}') \approx n_s \exp\{i\mathbf{k}(\mathbf{r} - \mathbf{r}') - (\mathbf{r} - \mathbf{r}')^2 / 2\xi_1^2\}, \qquad (7.4)$$

where

$$\mathbf{k} = \alpha_0(F/8\gamma w')\mathbf{b} \qquad (7.5)$$

is the wave vector and

$$\xi_1 = (2\alpha_0)^{1/2} \qquad (7.6)$$

is the dephasing length. Clearly, Eq. (7.4) implies the asymptotic decay formula (7.2) where $\eta^2 = n_s$. Inserting Eq.

(7.3) into Eq. (7.5) we find that $\mathbf{k}$ is exactly the average wave vector (A41) which we have calculated in the Appendix. By using $\bar{r}_1 = \xi^{-2}\rho_1$ and $\rho_1 = \sigma^{1/3}\zeta$ we find that the dephasing length (7.6) can be written in the form

$$\xi_1 = \xi[\tfrac{4}{3}(-\zeta)]^{1/4}\sigma^{-1/6}. \qquad (7.7)$$

This formula is suitable for a numerical evaluation of ξ_1 because ζ and σ are two of the seven dimensionless parameters, which are determined in Sec. IV. In Fig. 6 the dephasing length ξ_1 is shown as dashed line. We note that ξ_1 is defined only in the superfluid region for $\Delta T \lesssim \Delta T_\lambda(Q)$. It turns out that ξ_1 is always larger than ξ. While the correlation length ξ decreases with increasing distance from criticality, the dephasing length ξ_1 increases.

By using the asymptotic formulas of Sec. V B an asymptotic formula for ξ_1 can be derived. Eliminating the amplitude A from Eqs. (5.10) and (5.11) we obtain

$$\sigma^{-1/6} \approx (-\zeta)^{1/2} \frac{A_d}{8u[\tau]} \frac{g_0 k_B T_\lambda}{Q\xi^{d-1}}. \qquad (7.8)$$

Consequently, from Eq. (7.7) we obtain

$$\xi_1 \approx [\tfrac{4}{3}(-\zeta)^3]^{1/4} \frac{A_d}{8u[\tau]} \frac{g_0 k_B T_\lambda}{Q\xi^{d-2}}. \qquad (7.9)$$

Since ζ is nearly constant, the leading dependences on ΔT and Q are governed by

$$\xi_1 \sim Q^{-1}\xi^{-(d-2)} \sim Q^{-1}(-\Delta T)^{(d-2)\nu}. \qquad (7.10)$$

This asymptotic formula clearly indicates that the dephasing length ξ_1 diverges in the limit $Q \rightarrow 0$. Thus in thermal equilibrium where $Q = 0$ the second correlation length ξ_1 is infinite as expected, which means that in this case vortices are not present.

In the Appendix we have calculated the Green's function $G(\mathbf{r}, \mathbf{r}')$ and the related quantities n_s and J_s approximately by linearizing the parameters r_1 and Δr locally with respect to the space variable $\mathbf{r}$ according to Eqs. (A12) and (A13). Since r_1 and Δr are related to the temperature profiles $\Delta T(z) = T(z) - T_\lambda(z)$ and $T(z)$, respectively, and since $T_\lambda(z)$ is always a linear function in z, the validity of the approximation is proven if the curvature $\partial_z^2 T$ of the temperature profile is negligible compared to the gradient $\partial_z T$. For this purpose we define

$$\xi_2 = |\partial_z T| / |\partial_z^2 T| \qquad (7.11)$$

which may be viewed as the characteristic length scale for the variations of the temperature profile $T(z)$ with respect to the space coordinate z. In Fig. 6 the characteristic length ξ_2 is shown as dotted line. The curvature of $T(z)$ is negligible if ξ_2 is considerably larger than the intrinsic correlation lengths ξ and ξ_1 of the helium. In Fig. 6 the dotted line is considerably above the solid line and the dashed line for temperatures ΔT sufficiently far away from $\Delta T_\lambda(Q)$. Consequently, the criterion for the validity of our approximation is satisfied in the normal-fluid region and in the superfluid region sufficiently far away from the superfluid–normal-fluid interface. Close to the interface all three correlation lengths ξ, ξ_1, and

ξ_2 have the same order of magnitude so that here the curvature of $T(z)$ is important and our approximation is strictly speaking invalid. However, since nothing unusual is observed here, we believe that our theory yields reasonable and reliable interpolations for the physical quantities close to the interface.

The dotted line in Fig. 6 represents the characteristic length ξ_2 for a heat flow in zero gravity. Similar results for ξ_2 are obtained if we insert the temperature profile of a vertical heat flow in gravity. Deviations are expected for temperatures $\Delta T \lesssim \Delta T_1(Q)$. In gravity we find a somewhat smaller ξ_2, except for the downwards heat flow if ΔT is close to $\Delta T_1(Q)$. In the latter case ξ_2 diverges in the limit $\Delta T \rightarrow \Delta T_1(Q)$ which means that for the SOC state the approximation is exactly valid. Eventually, it turns out that the criterion for the validity of our approximation for calculating $G(\mathbf{r}, \mathbf{r}')$, n_s, and J_s is not affected significantly by gravity.

VIII. ENTROPY AND SPECIFIC HEAT

In model F the field variable $m(\mathbf{r}, t)$ represents a fluctuating entropy density divided by k_B. For this reason the local entropy density is defined by

$$S = S_0 + k_B \langle m \rangle, \tag{8.1}$$

where S_0 is a constant. Thus the average $\langle m \rangle$ must be evaluated. From the free-energy functional (2.3) we derive

$$\left\langle \frac{\delta H}{\delta m} \right\rangle = \chi_0^{-1} \langle m \rangle + \gamma_0 \langle |\psi|^2 \rangle - h_0. \tag{8.2}$$

We insert this quantity into Eq. (3.29), replace $\langle |\psi|^2 \rangle = n_s$, and obtain

$$r_0(z) = \tau_0(z) + 2\chi_0 \gamma_0^2 n_s + 2\gamma_0 \langle m \rangle. \tag{8.3}$$

From Eq. (3.31) we obtain $n_s = (4u_0)^{-1}[r_1(z) - r_0(z)]$. We resolve Eq. (8.3) with respect to $\langle m \rangle$ and then obtain the entropy

$$S = S_0 + k_B (2\gamma_0)^{-1} \left\{ -\tau_0(z) + r_0(z) \right. $$
$$\left. + \frac{\chi_0 \gamma_0^2}{2u_0}[r_0(z) - r_1(z)] \right\}. \tag{8.4}$$

Within our approximation in Secs. II and III we find $r_0(z) = r_1(z) = 0$ at the critical point $(\Delta T, Q, g) = (0,0,0)$. Hence

$$S_\lambda = S_0 - k_B (2\gamma_0)^{-1} \tau_0(z) \tag{8.5}$$

is the entropy density at $T = T_\lambda$ in thermal equilibrium and zero gravity. We define the entropy difference $\Delta S = S - S_\lambda$ as the deviation from the entropy at criticality S_λ. Then, from Eqs. (8.4) and (8.5) we obtain

$$\Delta S = k_B \frac{r_0(z)}{2\gamma_0} \left[1 + \frac{\chi_0 \gamma_0^2}{2u_0} \left(1 - \frac{r_1(z)}{r_0(z)} \right) \right]. \tag{8.6}$$

While S_λ is a constant, $\Delta S = \Delta S(\Delta T, Q)$ is strongly influenced by the critical fluctuations near the superfluid transition. For this reason, we must renormalize the entropy ΔS

and apply the RG theory. In analogy to the field variable $m(\mathbf{r}, t)$ the entropy is renormalized by[13]

$$\Delta S = (\chi_0 Z_m)^{1/2} \Delta S_{\text{ren}}. \tag{8.7}$$

In Eq. (8.6) we replace the bare model-F parameters by the renormalized counterparts by using Eqs. (4.1), (4.5), and (4.6). As a result we obtain the renormalized entropy

$$\Delta S_{\text{ren}} = k_B \left(\frac{A_d}{\mu^\epsilon} \right)^{1/2} \frac{r(z)}{2\gamma} \left[1 + \frac{\gamma^2}{2u} \left(1 - \frac{r_1(z)}{r(z)} \right) \right]. \tag{8.8}$$

Within the Hartree approximation all Z factors cancel, where an expansion with respect to the coupling parameters is not necessary. By resolving Eq. (4.25) with respect to $\chi_0 Z_m$ we obtain the renormalization factor of Eq. (8.7) as

$$(\chi_0 Z_m)^{1/2} = (A_d \mu^d)^{1/2} [2\tau\gamma]^{-1}. \tag{8.9}$$

We replace $r(z)$ and $r_1(z)$ by the dimensionless variables ρ and ρ_1 according to Eqs. (4.11) and (4.13). We apply the RG theory to Eqs. (8.7)–(8.9) by replacing $\mu \rightarrow \mu l = \xi^{-1}$, $u \rightarrow u[\tau]$, $\gamma \rightarrow \gamma[\tau]$, etc., so that now all dimensionless coupling parameters depend on the RG flow parameter τ. Combining the resulting three equations together we eventually obtain the entropy difference

$$\Delta S = k_B \frac{A_d}{4\tau\xi^d} \rho \left[\frac{1}{\gamma[\tau]^2} + \frac{1}{2u[\tau]} \left(1 - \frac{\rho_1}{\rho} \right) \right]. \tag{8.10}$$

Equation (8.10) is the final formula which can be used for numerical evaluation of the entropy density $S = S_\lambda + \Delta S$. There are no adjustable parameters present in this formula. The needed dimensionless parameters τ, ρ, and ρ_1 and the correlation length $\xi = \xi(\tau)$ were determined in Sec. IV. We note that Eq. (8.10) was derived within the Hartree approximation. It is not restricted to the physical situation considered in this paper where the helium is influenced by a heat current and gravity. The formula can be applied also to other physical situations as, e.g., rotating helium whenever the Hartree approximation is used.

The entropy ΔS is a static quantity so that nonasymptotic effects of the dynamic RG theory are very small. For this reason, close to criticality Eq. (8.10) can be evaluated asymptotically by using the asymptotic formulas $\xi = \xi_0 \tau^{-\nu}$, $u[\tau] \approx u^* = 0.0362$, and

$$\frac{1}{\gamma[\tau]^2} = \frac{4\nu}{\alpha}(1 - b\tau^\alpha), \tag{8.11}$$

where $\nu = 0.671$ and $\alpha = 2 - d\nu = -0.013$ (see Refs. 13 and 30). Equation (8.11) is obtained by solving the RG equation for $\gamma[\tau]$ asymptotically. Since $\gamma[\tau]$ is a known function,[13] b is a known constant (which actually is close to unity). Now, inserting the asymptotic formulas into Eq. (8.10) we eventually obtain the entropy density

$$S = S_\lambda + t(B + \tilde{A}\{(4\nu/\alpha) + E[u^*]\}\tau^{-\alpha}), \tag{8.12}$$

where

$$t = \tau\rho = \Delta T/T_\lambda, \tag{8.13}$$

$$E[u] = (2u)^{-1}[1 - \rho_1/\rho], \tag{8.14}$$

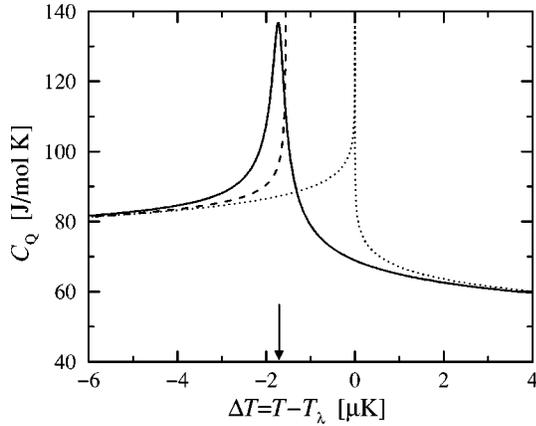FIG. 7. The specific heat $C_Q(\Delta T, Q)$ as a function of ΔT for the constant heat current $Q = 42.9$ μW/cm^2. Our theoretical result obtained from Eqs. (8.12) and (8.17) is shown as solid line. The dashed line represents C_Q of the previous theory,[37] where vortices were neglected. For comparison we have plotted the specific heat in thermal equilibrium for $Q = 0$ as dotted line. The arrow indicates $\Delta T_\lambda(Q)$.

$$\tilde{A} = k_B A_d / 4 \xi_0^d, \tag{8.15}$$

$$B = \tilde{A}(-4\nu/\alpha)b. \tag{8.16}$$

The specific heat C is obtained by differentiation of the entropy S with respect to temperature according to

$$C = T_\lambda \frac{\partial S}{\partial T} = \frac{\partial S}{\partial t}. \tag{8.17}$$

From our experience the best way to calculate the specific heat is first to calculate the entropy S by Eqs. (8.10) or (8.12) and then to determine the specific heat C by numerical differentiation via Eq. (8.17). (The alternative way, to differentiate the bare entropy (8.4) first with respect to $r_0(z)$ and then to apply the RG theory, is less reliable and yields artifacts, so that it should not be used.) While the constants $\tilde{A}$ and B are given by Eqs. (8.15) and (8.16), we can alternatively determine these constants by fitting the specific heat in thermal equilibrium to the data of the newest experiment,[32] which was performed in microgravity in space. In this way we obtain $\tilde{A} = 2.22$ J/mol K and $B = 456$ J/mol K. Since in the experiments the *molar* specific heat is measured, we have multiplied the constants by the molar volume V_λ, which for saturated vapor pressure is[31] $V_\lambda = 27.38$ cm^3/mol.

The specific heat C depends on the thermodynamic variable which is kept constant when performing the differentiation with respect to temperature in Eq. (8.17). Since we consider liquid ^{4}He in the presence of a constant heat flow, the heat current Q is the natural variable which should be kept constant. For this reason we calculate C_Q at constant Q. In Fig. 7 $C_Q = C_Q(\Delta T, Q)$ is plotted as a function of ΔT for $Q = 42.9$ μW/cm^2, i.e., the same heat current as in Figs. 3 and 6. Our theoretical result is shown as solid line. For comparison, the specific heat in thermal equilibrium at $Q = 0$ is shown as dotted line. While in thermal equilibrium the specific heat is singular at $\Delta T = 0$, for nonzero Q we find a
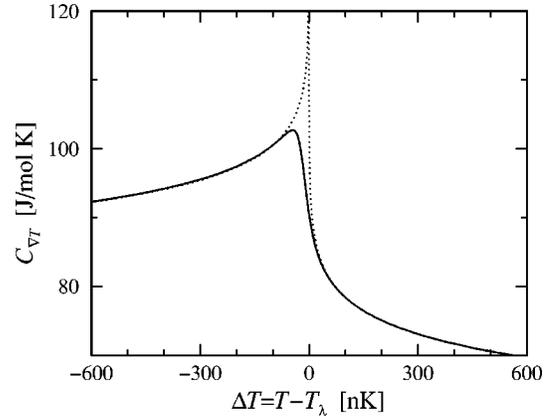

FIG. 8. The specific heat $C_{\nabla T}(\Delta T, Q)$ as a function of ΔT for the self-organized critical (SOC) state where the temperature gradient is fixed by gravity according to $\partial_z T = \partial_z T_\lambda = -1.273$ μK/cm. The solid line represents our theoretical result obtained from Eqs. (8.12) and (8.17). For comparison the specific heat in thermal equilibrium is shown as dotted line.

smooth curve for C_Q which exhibits a strong maximum located at $\Delta T_\lambda(Q)$. We note that the temperature $T(z)$ is space dependent, so that the specific heat $C_Q(z)$ is also space dependent and must be interpreted as a local quantity.

Within the framework of the previous theory,[4] the specific heats C_{V_s} and $C_Q = C_{J_s}$ were calculated and a similar formula like Eq. (8.12) was obtained for the entropy.[37] In Fig. 7 the specific heat C_Q of the previous theory is shown as dashed line. Since the heat flow is metastable below and unstable above $\Delta T_\lambda(Q)$, the dashed line is defined only for $\Delta T < \Delta T_\lambda(Q)$. The specific heat C_Q is enhanced by the nonzero Q and diverges[46] at $\Delta T_\lambda(Q)$. Experiments to measure C_Q at constant Q are in progress.[38] An enhancement of the specific heat by a nonzero heat current was found just recently.

The self organized critical (SOC) state represents an ideal system for measuring thermodynamic quantities like the specific heat because it is homogeneous in space over a large region. In this case the temperature gradient is fixed by gravity according to $\partial_z T = \partial_z T_\lambda = -1.273$ μK/cm. Thus in the SOC state the specific heat $C_{\nabla T}$ at constant-temperature gradient will be measured. We calculate $C_{\nabla T}$ from Eq. (8.17) by inserting the entropy (8.12) and keeping $\partial_z T = \partial_z T_\lambda$ constant when performing the numerical differentiation, while the heat current Q is varied appropriately. The result is shown in Fig. 8 as solid line. For comparison, the equilibrium specific heat is shown as dotted line. Clearly, the nonzero temperature gradient $\partial_z T = \partial_z T_\lambda$ of the SOC state induced by gravity implies a rounding of the critical singularity. The solid line is smooth and exhibits a maximum at $\Delta T_g = -45$ nK. While in Fig. 7 the maximum of C_Q is very strong and enhanced, here in Fig. 8 the maximum of $C_{\nabla T}$ is moderate and just represents a smooth and round interpolation of the equilibrium specific heat near criticality. The temperature scale in Fig. 8 indicates that nano-Kelvin resolution is sufficient for a measurement of $C_{\nabla T}$. Thus the rounded temperature dependence of $C_{\nabla T}$ should be accessible by present-day experiments. Since gravity is needed for the realization of the SOC state, the experiment should be performed on earth.

IX. VORTICES AND MUTUAL FRICTION

While our theory does not include vortices explicitly, here we present some arguments, which support that our theory includes the effect of vortices implicitly. In Sec. V we have calculated a finite thermal conductivity λ_T for $\Delta T \lesssim \Delta T_\lambda(Q)$ which implies dissipation of the heat current Q in the superfluid state. Since the heat is transported convectively by the superfluid–normal-fluid counterflow, a superfluid current with a velocity v_s is induced in the opposite direction of the heat flow. The superfluid velocity v_s is related to the phase of the order parameter field $\psi(\mathbf{r},t)$, so that the dissipation of the superfluid current is necessarily related to the creation of vortices. Thus since our theory describes dissipation, it must include vortices in some way.

Gorter and Mellink[15] investigated mutual friction of the counterflow experimentally and proposed the mutual-friction force density

$$f = A\rho_n\rho_s(v_s - v_n)^3, \qquad (9.1)$$

where A is the so called Gorter-Mellink coefficient which may be a function of temperature but which should be independent of the velocities v_s and v_n. The force density (9.1) was added to the hydrodynamic equations of the two-fluid model [see Eqs. (8) and (9) in Ref. 15]. For a stationary counterflow the relation

$$\frac{\rho_n\rho_s}{\rho}s_\lambda\partial_z T = A\rho_n\rho_s(v_s - v_n)^3 \qquad (9.2)$$

was found, where the pressure gradient is neglected close to criticality. This relation implies $\partial_z T \sim (v_s - v_n)^3$ and means that the temperature gradient induced by the mutual friction is proportional to the third power of the counterflow velocity. By experimental and theoretical considerations Vinen[16] showed that the ansatz (9.1) is related to a turbulent superfluid flow which generates a tangle of vortices which imply the mutual friction. A statistical theory for the superfluid turbulence in a homogeneous counterflow was developed by Schwarz.[39] This latter theory supports Eqs. (9.1) and (9.2). The Gorter-Mellink coefficient A was calculated[39] for temperatures in the interval $1.2 < T < 2.05$ K and agreement with the experiments[16,40] was found (see also the review by Tough[41]).

Now, here we show that the ansatz of Gorter and Mellink [Eq. (9.1)] can be derived from model F by our approximation. To do this, we resolve Eq. (9.2) with respect to A, obtain

$$A = \frac{s_\lambda}{\rho}\frac{\partial_z T}{(v_s - v_n)^3}, \qquad (9.3)$$

and insert the results of our calculations. The coefficient A must be proven to be independent of Q and $v_s - v_n$. Near criticality v_n can be neglected because it is much smaller than v_s. The superfluid velocity v_s is related to the wave number k of the order parameter by $v_s = \hbar k/m_4$. The entropy per mass s_λ is related to the model-F parameter g_0 by[31] $s_\lambda = (\hbar/m_4)(g_0/T_\lambda)$. The temperature gradient $\partial_z T$ is related to the thermal conductivity λ_T by Eq. (6.1). Then, from Eq. (9.3) we obtain the Gorter-Mellink coefficient

$$A = \left(\frac{m_4}{\hbar}\right)^2\frac{g_0}{\rho_\lambda T_\lambda}\frac{Q}{\lambda_T k^3}. \qquad (9.4)$$

In the previous theory[4] the heat current Q was calculated as a function of the wave number k where the heat flow is metastable and dissipation by creation of vortices is neglected. In the superfluid region sufficiently well below $\Delta T_\lambda(Q)$ the dissipation is small so that the result for $Q = Q(\Delta T,k)$ of Ref. 4 may be used to replace k by Q. In this region, $Q = Q(\Delta T,k)$ is approximately a linear function of k given by

$$Q = \frac{g_0 k_B T_\lambda}{\xi^{d-2}}A_d\left(\frac{1}{8u[\tau]}+\frac{1}{d}\right)k. \qquad (9.5)$$

Consequently, we obtain

$$A = \left(\frac{m_4}{\hbar}\right)^2\frac{g_0}{\rho_\lambda T_\lambda}\frac{1}{\lambda_T Q^2}\left[\frac{g_0 k_B T_\lambda}{\xi^{d-2}}A_d\left(\frac{1}{8u[\tau]}+\frac{1}{d}\right)\right]^3. \qquad (9.6)$$

The last factor $[\cdots]$ does not depend explicitly on Q. It only depends on the RG flow parameter τ via $\xi = \xi_0\tau^{-\nu}$ where $u[\tau] \approx u^* = 0.0362$. Now, inserting the asymptotic formula (5.13) for the thermal conductivity λ_T we clearly see that the heat current Q cancels. Neglecting the one-loop contribution in the heat-current formula (9.5) we obtain the Gorter-Mellink coefficient

$$A \approx \left(\frac{m_4}{\hbar}\right)^2\frac{g_0}{\rho_\lambda}\sqrt{\frac{12}{(-\zeta)^{3/2}}}\frac{4\gamma[\tau]w'[\tau]}{F[\tau]}\tau\xi^2 \qquad (9.7)$$

which does not depend explicitly on Q. A weak indirect Q dependence is included in the dimensionless variable ζ, which represents the nonasymptotic effects of the dynamic RG theory. In leading order we find the asymptotic formula

$$A \sim \tau\xi^2 \sim (-\Delta T)^{1-2\nu}. \qquad (9.8)$$

This result proves that within the approximation of our theory the ansatz of Gorter and Mellink is correct and can be derived from model F.

Equation (9.6) can be used for an explicit calculation of the Gorter-Mellink coefficient $A = A(\Delta T,Q)$ as a function of $\Delta T = T - T_\lambda$ and Q, where our result for $\lambda_T = \lambda_T(\Delta T,Q)$ from Sec. V is inserted. While most constants and parameters are known, we additionally need $m_4/\hbar = 6320$ s/cm^2 and the density ρ_λ of the helium at T_λ, which at saturated vapor pressure is given by[31] $\rho_\lambda = N_A m_4/V_\lambda = 0.146$ g/cm^3. In Fig. 9 our theoretical prediction for A is shown versus ΔT double logarithmically for several heat currents Q which change by a factor of 10 between each curve. The lowest and most left curve corresponds to the smallest heat current $Q = 1$ pW/cm^2, while the highest and most right curve corresponds to the largest heat current $Q = 1$ mW/cm^2. Since the helium is superfluid only for $\Delta T \lesssim \Delta T_\lambda(Q)$, all curves have an endpoint on the left-hand side.

If the cancellation of Q in Eq. (9.6) is perfect, then the curves in Fig. 9 would lie all on the same line. This, however, is not the case. The nonasymptotic effects of the dynamic RG theory imply that $A(\Delta T,Q)$ depends weakly on Q. While the heat current Q is varied over 9 decades, A
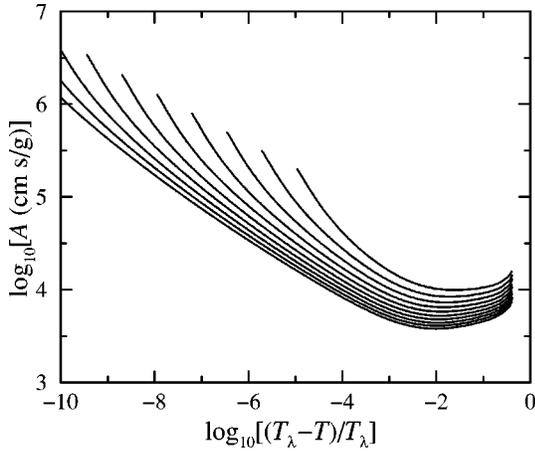
FIG. 9. The Gorter-Mellink coefficient A obtained from Eq. (9.6) as a function of temperature for several heat currents between $Q = 1$ pW/cm^2 and 1 mW/cm^2 (curves from left to right, heat currents increase by a factor of 10, respectively). The left ends of the curves are located close to the superfluid transition at $\Delta T_\lambda(Q)$.

changes by a factor of 3 to 10 or by 0.5 to 1.0 decades. Consequently, we approximately find

$$A \sim Q^y \sim (v_s - v_n)^y \qquad (9.9)$$

with an exponent y between 0.05 and 0.1. This result slightly modifies the mutual friction force (9.1) of Gorter and Mellink into

$$f \sim (v_s - v_n)^\phi \qquad (9.10)$$

with the exponent $\phi = 3 + y$ between 3.05 and 3.1.

The Gorter-Mellink coefficient A was measured as a function of temperature by Vinen.[16] The value $A \approx 200$ cm s/g was obtained for $\Delta T \approx -0.1$ K, which can be extrapolated to $A \sim 600$ cm s/g for $\Delta T \sim -0.01$ K. Similar values for A were obtained also in later experiments, which are reviewed in Ref. 41. On the other hand, the lowest values, that our theory predicts, are about $A \sim 10^4$ cm s/g for $\Delta T \sim -0.01$ K. Thus our theoretical prediction for A is about one or two decades larger than the experimental values. Furthermore, A can be extracted from the experimental data of Baddar et al.[17] by inserting the power-law formula (5.15) for the thermal conductivity λ_T into Eq. (9.6). Again, our theoretical prediction is about a factor of 20 larger than the experimentally observed values. Thus we conclude that our theory has a tendency to overestimate the magnitude of the dissipation and mutual friction due to creation of vortices. On the other hand, the experimental data of Ref. 17 imply the exponent $\phi = 3.53$ for the mutual friction force (9.10), which is considerably larger than the exponent proposed by Gorter and Mellink[15] and obtained from our theory.

The discrepancies are possibly due the number of vortices in the helium in the presence of a homogeneous heat flow Q, because the number of vortices appears to be an unknown and uncontrolled quantity in theory and experiment. In rotating helium mutual friction can by studied in a much more controlled fashion,[42] because in this case the number of vortices is related to the rotation frequency. Here the mutual friction is described by the Vinen coefficients[42] B and B'. These coefficients have been measured experimentally (see

Ref. 43 for review) and also calculated within model F in renormalized mean-field theory[44] by considering the motion of a single vortex line. We have applied our theory (the Hartree approximation combined with the RG theory) also to rotating helium and find the coefficients[45] $B = (4m_4/\hbar)\Gamma'[\tau]$ and $2 - B' = (4m_4/\hbar)\Gamma''[\tau]$. While these results are indeed simple, they have the same order of magnitude than the coefficients B and B' of the previous theory[44] and also of the experiments.[43] The agreement is better for B than for B'. Thus we conclude that our present theory indeed includes the effects of vortices. However, since a simple approximation is applied, the Hartree approximation (see Fig. 2), discrepancies are expected. Nevertheless, for the Vinen coefficients B and B' the discrepancies are much smaller than for the Gorter-Mellink coefficient A.

X. CONCLUSIONS

We have presented a renormalization-group (RG) theory based on model F for liquid ^{4}He near the superfluid transition in the presence of a heat current Q and gravity. The fundamental concept is a self-consistent approximation, which in quantum many-particle theory is known as the Hartree approximation, combined with the RG theory. While above T_λ the previous theory of Ref. 3 is recovered for a heat flow in normal-fluid ^{4}He, below T_λ in the superfluid state our theory predicts dissipation of the heat current and mutual friction of the related superfluid–normal-fluid counterflow.

We derived the ansatz of Gorter and Mellink[15] for the mutual friction force and found several indications that our approach includes vortices indirectly. However, our approach appears to overestimate the magnitude of the dissipation by vortex creation considerably compared to the experimental observations. This discrepancy is probably due to the number of vortices in the superfluid helium which appears to be an uncertain and very sensitive quantity strongly influenced by the kind of the approximation and also by the experimental conditions. Further theoretical and experimental work is necessary to clarify the discrepancies.

Besides the correlation length $\xi = \xi_0 \tau^{-\nu}$, which is the conventional length scale of the RG theory, in the superfluid state we find a second characteristic length ξ_1 which describes the decay of the correlations by dephasing of the order parameter field $\psi(\mathbf{r})$ caused by vortices. The dephasing length ξ_1 may be viewed as the average distance between the vortices. It is much larger than ξ (see Fig. 6) and approximately given by $\xi_1 \approx a Q^{-1} \tau^{+\nu}$ where $\tau = -2\Delta T/T_\lambda$ and $a \approx 1.0$ mW/cm. Thus for superfluid ^{4}He in confined geometries we expect interesting effects when the dephasing length ξ_1 is as large as the geometry and hits the boundary walls. Future theoretical and experimental investigations should study the influence of vortices in superfluid ^{4}He on finite-size effects and on boundary effects. Unexpected results for the thermal conductivity in confined geometries and for the Kapitza resistance may possibly be found, which are caused by the second characteristic length ξ_1.

valuable discussions. Furthermore, I would like to thank Dr. M. Lee, Dr. U. Israelsson, and Dr. D. Strayer for the invitation to the 1998 NASA/JPL workshop on fundamental physics in microgravity, held in Oxnard, CA, where many questions about the relation between theory and experiment were discussed and clarified.

APPENDIX: INTEGRAL REPRESENTATION FOR THE GREEN'S FUNCTION

In Sec. III and in Ref. 3 we have evaluated $n_s = \langle |\psi|^2 \rangle$ and $\mathbf{J}_s = \langle \text{Im}[\psi^* \boldsymbol{\nabla} \psi] \rangle$ explicitly, which eventually are expressed in terms of an integral by Eqs. (4.27) and (4.28). While for our purposes we only need n_s and $\mathbf{J}_s$, it is also possible to evaluate the complete matrix Green's function G explicitly. This Green's function is defined by Eq. (3.18). First of all, we need the inverse of the operator matrix (3.17) which is given by

$$(K_{\alpha\beta}^{-1}) = \begin{pmatrix} 0 & 2(L^+)^{-1} \\ 2L^{-1} & 4\Gamma'L^{-1}(L^+)^{-1} \end{pmatrix}. \qquad (A1)$$

Since we intend to evaluate the renormalized Green's function, we use Eq. (4.4) for the operator L, where all model-F parameters are replaced by the renormalized parameters.

Here we consider the Green's function $\langle \psi\psi^* \rangle$ which is given by the lower-right element G_{22} of the matrix Green's function G. From Eqs. (3.18) and (A1) we obtain

$$\langle \psi(\mathbf{r},t)\psi^*(\mathbf{r}',t') \rangle = 4\Gamma'L^{-1}(L^+)^{-1}\delta(\mathbf{r}-\mathbf{r}')\delta(t-t'). \qquad (A2)$$

We represent the inverse operators L^{-1} and $(L^+)^{-1}$ as integrals of exponential functions so that the Green's function is rewritten as

$$\langle \psi(\mathbf{r},t)\psi^*(\mathbf{r}',t') \rangle = 4\Gamma' \int_0^\infty d\alpha \int_0^\infty d\beta\, e^{-\alpha L}e^{-\beta L^+}$$
$$\times \delta(\mathbf{r}-\mathbf{r}')\delta(t-t'). \qquad (A3)$$

We decompose the operators in the exponentials into time-dependent and space-dependent parts according to

$$-\alpha L = -\alpha\partial_t + \alpha A, \qquad (A4)$$

$$-\beta L^+ = +\beta\partial_t + \beta B, \qquad (A5)$$

where

$$A = -\{\Gamma[r_1 - \boldsymbol{\nabla}^2] - i(g/2\gamma)\Delta r\}, \qquad (A6)$$

$$B = -\{\Gamma^*[r_1 - \boldsymbol{\nabla}^2] + i(g/2\gamma)\Delta r\}. \qquad (A7)$$

Since ∂_t commutes with the space-dependent operators A and B, we obtain

$$\langle \psi(\mathbf{r},t)\psi^*(\mathbf{r}',t') \rangle = 4\Gamma' \int_0^\infty d\alpha \int_0^\infty d\beta\, e^{\alpha A}e^{\beta B}$$
$$\times \delta(\mathbf{r}-\mathbf{r}')e^{(-\alpha+\beta)\partial_t}\delta(t-t'). \qquad (A8)$$

The time-dependent factor is evaluated by the Taylor series according to

$$e^{(-\alpha+\beta)\partial_t}\delta(t-t') = \delta(-\alpha+\beta+t-t'). \qquad (A9)$$

The space-dependent factor is more complicated and can be evaluated by using the formula

$$e^A e^B = \exp\{A+B+\tfrac{1}{2}[A,B]$$
$$+\tfrac{1}{12}([A,[A,B]]-[B,[A,B]])$$
$$-\tfrac{1}{24}[B,[A,[A,B]]]+\cdots\}. \qquad (A10)$$

1. Equal time Green's function

For simplicity we set $t' = t$, and from now on we consider only the equal time Green's function. The integral over β can be evaluated easily by the delta function (A9) so that we obtain

$$G(\mathbf{r},\mathbf{r}') = \langle \psi(\mathbf{r},t)\psi^*(\mathbf{r}',t) \rangle$$
$$= 4\Gamma' \int_0^\infty d\alpha\, e^{\alpha A}e^{\alpha B}\delta(\mathbf{r}-\mathbf{r}'). \qquad (A11)$$

For a successful calculation of the space-dependent integrand the series in the exponential on the right-hand side of Eq. (A10) must be finite, which means that only a finite number of the commutators may be nonzero. For this reason, we assume r_1 and Δr to be linear functions of the space coordinate $\mathbf{r}$ given by

$$r_1 = a_1 + \mathbf{b}_1\mathbf{r}, \qquad (A12)$$

$$\Delta r = a + \mathbf{b}\mathbf{r}, \qquad (A13)$$

where a_1 and a are constants and $\mathbf{b}_1$ and $\mathbf{b}$ are constant vectors. In general, r_1 and Δr are nonlinear functions of $\mathbf{r}$. In this case r_1 and Δr must be linearized locally so that Eqs. (A12) and (A13) are taken as an approximation where $\mathbf{b}_1$ and $\mathbf{b}$ are the respective gradients at the space point $\mathbf{R} = \frac{1}{2}(\mathbf{r} + \mathbf{r}')$. In the main text of this paper we assume $r_1(z)$ and $\Delta r(z)$ to be functions of the coordinate z only so that the gradients $\mathbf{b}_1 = r_1'\mathbf{e}_z$ and $\mathbf{b} = \Delta r'\mathbf{e}_z$ are vectors in z direction. However, this latter assumption is not necessary here.

Now, Eqs. (A12) and (A13) imply the commutators $[r_1,\boldsymbol{\nabla}^2] = -2\mathbf{b}_1\boldsymbol{\nabla}$ and $[\Delta r,\boldsymbol{\nabla}^2] = -2\mathbf{b}\boldsymbol{\nabla}$. Consequently, we find

$$[A,B] = -i(g\Gamma'/\gamma)2\mathbf{b}\boldsymbol{\nabla}, \qquad (A14)$$

$$[A,[A,B]] = -2i(g\Gamma'/\gamma)\{\Gamma\mathbf{b}_1\mathbf{b}-i(g/2\gamma)\mathbf{b}^2\}, \qquad (A15)$$

$$[B,[A,B]] = -2i(g\Gamma'/\gamma)\{\Gamma^*\mathbf{b}_1\mathbf{b}+i(g/2\gamma)\mathbf{b}^2\}. \qquad (A16)$$

The double commutators (A15) and (A16) are c numbers because $\mathbf{b}_1$ and $\mathbf{b}$ are assumed to be constant. Hence all higher-order commutators are zero so that the series in the exponential on the right-hand side of Eq. (A10) is finite. Eventually, inserting the commutators (A14)–(A16) into Eq. (A10) we obtain

$$e^{\alpha A}e^{\alpha B}=\exp\left\{-2\Gamma'\alpha[r_1-\mathbf{\nabla}^2]-i(2\Gamma'\alpha)^2\frac{g}{4\gamma\Gamma'}\mathbf{b}\mathbf{\nabla}\right.$$
$$+\frac{1}{12}(2\Gamma'\alpha)^3\left[2\frac{\Gamma''}{\Gamma'}\left(\frac{g}{4\gamma\Gamma'}\mathbf{b}\right)\mathbf{b}_1\right.$$
$$\left.\left.-4\left(\frac{g}{4\gamma\Gamma'}\mathbf{b}\right)^2\right]\right\}. \tag{A17}$$

This formula is exact if r_1 and Δr are linear functions in $\mathbf{r}$ given by Eqs. (A12) and (A13).

Next, we consider the operators $C=-2\Gamma'r_1$ and $D=2\Gamma'(\mathbf{\nabla}-i\mathbf{k})^2$ where $\mathbf{k}$ is a constant wave vector. We find the commutators

$$[C,D]=(2\Gamma')^2 2\mathbf{b}_1(\mathbf{\nabla}-i\mathbf{k}), \tag{A18}$$

$$[C,[C,D]]=(2\Gamma')^3 2\mathbf{b}_1^2, \tag{A19}$$

$$[D,[C,D]]=0. \tag{A20}$$

Since the double commutators are c numbers, again the higher-order commutators are zero. Thus from Eq. (A10) we obtain the formula

$$e^{\alpha C}e^{\alpha D}=\exp\{-2\Gamma'\alpha[r_1-(\mathbf{\nabla}-i\mathbf{k})^2]$$
$$+(2\Gamma'\alpha)^2\mathbf{b}_1(\mathbf{\nabla}-i\mathbf{k})+\tfrac{1}{6}(2\Gamma'\alpha)^3\mathbf{b}_1^2\}. \tag{A21}$$

We choose the wave vector

$$\mathbf{k}=\Gamma'\alpha\left(\frac{g}{4\gamma\Gamma'}\mathbf{b}-i\mathbf{b}_1\right) \tag{A22}$$

and then rewrite Eq. (A21) as

$$e^{\alpha C}e^{\alpha D}=\exp\left\{-2\Gamma'\alpha[r_1-\mathbf{\nabla}^2]-i(2\Gamma'\alpha)^2\frac{g}{4\gamma\Gamma'}\mathbf{b}\mathbf{\nabla}\right.$$
$$\left.-\frac{1}{12}(2\Gamma'\alpha)^3\left[\mathbf{b}_1^2+3\left(\frac{g}{4\gamma\Gamma'}\mathbf{b}\right)^2\right]\right\}. \tag{A23}$$

Now, we clearly see that the operators in the exponentials on the right-hand sides of Eqs. (A17) and (A23) are equal up to an additive constant. Thus from comparison of Eqs. (A17) and (A23) we obtain the relation

$$e^{\alpha A}e^{\alpha B}=e^{-(2\Gamma'\alpha)^3 s}\cdot e^{\alpha C}e^{\alpha D}, \tag{A24}$$

where

$$s=-\frac{1}{12}\left[\mathbf{b}_1^2+2\frac{w''}{w'}\left(\frac{F}{4\gamma w'}\mathbf{b}\right)\mathbf{b}_1-\left(\frac{F}{4\gamma w'}\mathbf{b}\right)^2\right]. \tag{A25}$$

Here we have replaced Γ', Γ'', and g by the dimensionless ratios $w'=\Gamma'/\lambda$, $w''=\Gamma''/\lambda$, and $F=g/\lambda$. The first factor on the right-hand side of Eq. (A24) is just a constant, while the other exponential factors are operators. We insert the relation

(A24) together with the operators $C=-2\Gamma'(a_1+\mathbf{b}_1\mathbf{r})$ and $D=2\Gamma'(\mathbf{\nabla}-i\mathbf{k})^2$ into Eq. (A11) and then obtain the Green's function

$$G(\mathbf{r},\mathbf{r}')=4\Gamma'\int_0^\infty d\alpha\, e^{-2(\Gamma'\alpha)^3 s}e^{-2\Gamma'\alpha(a_1+\mathbf{b}_1\mathbf{r})}$$
$$\times e^{2\Gamma'\alpha(\mathbf{\nabla}-i\mathbf{k})^2}\delta(\mathbf{r}-\mathbf{r}'). \tag{A26}$$

We substitute $2\Gamma'\alpha\to\alpha$ and evaluate the last two factors by using the Gaussian integral and the Taylor series:

$$e^{\alpha(\mathbf{\nabla}-i\mathbf{k})^2}\delta(\mathbf{r}-\mathbf{r}')$$
$$=(4\pi\alpha)^{-d/2}\int d^d u\, e^{-(4\alpha)^{-1}\mathbf{u}^2+\mathbf{u}(\mathbf{\nabla}-i\mathbf{k})}\delta(\mathbf{r}-\mathbf{r}')$$
$$=(4\pi\alpha)^{-d/2}\int d^d u\ e^{-(4\alpha)^{-1}\mathbf{u}^2-i\mathbf{k}\mathbf{u}}\delta(\mathbf{r}-\mathbf{r}'+\mathbf{u})$$
$$=(4\pi\alpha)^{-d/2}e^{i\mathbf{k}(\mathbf{r}-\mathbf{r}')}e^{-(4\alpha)^{-1}(\mathbf{r}-\mathbf{r}')^2}. \tag{A27}$$

Thus inserting the wave vector (A22) with the proper subsitution for α and with g/Γ' replaced by F/w', for the Green's function we eventually obtain the formula

$$G(\mathbf{r},\mathbf{r}')=\frac{2}{(4\pi)^{d/2}}\int_0^\infty\frac{d\alpha}{\alpha^{d/2}}\exp\{-\alpha\bar{r}_1-\alpha^3 s\}$$
$$\times\exp\left(i\alpha\frac{F}{8\gamma w'}\mathbf{b}(\mathbf{r}-\mathbf{r}')-\frac{1}{4\alpha}(\mathbf{r}-\mathbf{r}')^2\right), \tag{A28}$$

where $\bar{r}_1=a_1+\tfrac{1}{2}\mathbf{b}_1(\mathbf{r}+\mathbf{r}')$. This formula is a simple integral, there are no operators in the integrand any more. Clearly, the Green's function depends on the average coordinate $\mathbf{R}=\tfrac{1}{2}(\mathbf{r}+\mathbf{r}')$ implicitly via $\bar{r}_1$ and explicitly on the relative coordinate $\Delta\mathbf{r}=\mathbf{r}-\mathbf{r}'$.

The integral (A28) has a similar but more general structure than the integral $\mathcal{F}_\alpha(\zeta)$ in Eq. (4.28). Thus it is possible to obtain n_s and J_s from the Green's function (A28). We find

$$n_s=\langle|\psi|^2\rangle=G(\mathbf{r},\mathbf{r})$$
$$=\frac{2}{(4\pi)^{d/2}}\int_0^\infty\frac{d\alpha}{\alpha^{d/2}}\exp\{-\alpha r_1-\alpha^3 s\} \tag{A29}$$

and

$$\mathbf{J}_s=\langle\text{Im}[\psi^*\mathbf{\nabla}\psi]\rangle=(2i)^{-1}[\mathbf{\nabla}-\mathbf{\nabla}']G(\mathbf{r},\mathbf{r}')|_{\mathbf{r}'=\mathbf{r}}$$
$$=\frac{F}{4\gamma w'}\frac{\mathbf{b}}{(4\pi)^{d/2}}\int_0^\infty\frac{d\alpha}{\alpha^{d/2-1}}\exp\{-\alpha r_1-\alpha^3 s\}. \tag{A30}$$

We identify $\mathbf{b}_1=r_1'\mathbf{e}_z$ and $\mathbf{b}=\Delta r'\mathbf{e}_z$ and find that s defined in Eq. (A25) is closely related to σ defined in Eq. (4.29). We substitute $\alpha=s^{-1/3}v$, identify $\zeta=s^{-1/3}r_1$, and rewrite n_s and J_s as

$$n_s=\frac{2}{(4\pi)^{d/2}}s^{(d-2)/6}\mathcal{F}_{(2-d)/2}(\zeta), \tag{A31}$$

$$J_s = \frac{F}{4\gamma w'} \frac{\Delta r'}{(4\pi)^{d/2}} s^{(d-4)/6} \mathcal{F}_{(4-d)/2}(\zeta), \qquad \text{(A32)}$$

where $\mathbf{J}_s = J_s \mathbf{e}_z$. By using the function $\Phi_\alpha(X)$ defined in Eq. (4.27) and identifying

$$\frac{1}{(4\pi)^{d/2}} = -\frac{1}{\epsilon} A_d \frac{1}{\Gamma(1-d/2)} \qquad \text{(A33)}$$

which may be viewed as the definition of the factor A_d, the formulas for n_s and J_s can be rewritten as

$$n_s = -\frac{2}{\epsilon} A_d \Phi_{-1+\epsilon/2}(X) r_1^{1-\epsilon/2}, \qquad \text{(A34)}$$

$$J_s = \frac{F}{2w'} \frac{\Delta r'}{2\gamma} \frac{1}{\epsilon} A_d (1-\epsilon/2) \Phi_{\epsilon/2}(X) r_1^{-\epsilon/2}, \qquad \text{(A35)}$$

where $X = -s/r_1^3$ and $\epsilon = 4-d$. Finally, replacing the renormalized couplings by the bare model-F parameters, we recover the formulas (3.24) and (3.25). Thus we have derived the formulas of Sec. III B for n_s and J_s once again. We note that the fundamental assumption here is the linear form of r_1 and Δr in Eqs. (A12) and (A13), which in general is an approximation. This assumption implies the special structure of the integrals in Eq. (A28) and in Eq. (4.28).

2. Fourier transformation of the Green's function and physical interpretation

The natural space variables of the equal time Green's function $G(\mathbf{r},\mathbf{r}')$ are the average coordinate $\mathbf{R} = \frac{1}{2}(\mathbf{r}+\mathbf{r}')$ and the relative coordinate $\Delta\mathbf{r} = \mathbf{r}-\mathbf{r}'$. This fact is clearly seen in Eq. (A28). Thus we may perform a Fourier transformation with respect to $\Delta\mathbf{r}$ and define the Fourier-transformed Green's function $\tilde{G}(\mathbf{R},\mathbf{k})$ by

$$G(\mathbf{r},\mathbf{r}') = \int \frac{d^d k}{(2\pi)^d} e^{i\mathbf{k}(\mathbf{r}-\mathbf{r}')} \tilde{G}(\mathbf{R},\mathbf{k}). \qquad \text{(A36)}$$

We apply this Fourier transformation to Eq. (A28) and then obtain

$$\tilde{G}(\mathbf{R},\mathbf{k}) = 2 \int_0^\infty d\alpha \, \exp\{-\alpha \bar{r}_1 - \alpha^3 s\}$$
$$\times \exp\left[-\alpha\left(\mathbf{k} - \alpha \frac{F}{8\gamma w'}\mathbf{b}\right)^2\right], \qquad \text{(A37)}$$

where $\bar{r}_1 = a_1 + \mathbf{b}_1 \mathbf{R}$. This Green's function is positive definite and may be viewed as a distribution function for the wave vector $\mathbf{k}$. We may define the average wave vector $\langle\mathbf{k}\rangle_\mathbf{R}$ at space point $\mathbf{R}$ by

$$\langle\mathbf{k}\rangle_\mathbf{R} = \int \frac{d^d k}{(2\pi)^d} \mathbf{k}\tilde{G}(\mathbf{R},\mathbf{k}) \left/ \int \frac{d^d k}{(2\pi)^d} \tilde{G}(\mathbf{R},\mathbf{k}). \right. \qquad \text{(A38)}$$

This formula can be rewritten in terms of the real-space Green's function $G(\mathbf{r},\mathbf{r}')$ as

$$\langle\mathbf{k}\rangle_\mathbf{R} = \{(2i)^{-1}[\boldsymbol{\nabla} - \boldsymbol{\nabla}']G(\mathbf{r},\mathbf{r}')\}/G(\mathbf{r},\mathbf{r}')|_{\mathbf{r}'=\mathbf{r}=\mathbf{R}}. \qquad \text{(A39)}$$

Thus by using Eqs. (A29)–(A32) we obtain

$$\langle\mathbf{k}\rangle_\mathbf{R} = \mathbf{J}_s/n_s = \frac{F}{8\gamma w'} \frac{\mathbf{b}}{-r_1} \frac{(-\zeta)\mathcal{F}_{\epsilon/2}(\zeta)}{\mathcal{F}_{-1+\epsilon/2}(\zeta)} \qquad \text{(A40)}$$

so that $\mathbf{J}_s = n_s\langle\mathbf{k}\rangle_\mathbf{R}$. While $\mathbf{J}_s$ is finite for $d<4$, n_s is ultraviolet divergent for $d>2$. As a consequence, for $d=3$ dimensions the average wave vector $\langle\mathbf{k}\rangle_\mathbf{R}$ is strictly speaking zero. In the superfluid state for temperatures well below T_λ we may use the asymptotic formula (4.44) for the function $\mathcal{F}_\alpha(\zeta)$. In this approximation the ultraviolet divergences are neglected so that we obtain a finite result for the average wave vector

$$\langle\mathbf{k}\rangle_\mathbf{R} = \frac{F}{8\gamma w'} \frac{\mathbf{b}}{-r_1} \frac{(-\zeta)^{3/2}}{3^{1/2}}. \qquad \text{(A41)}$$

Since the wave vector $\mathbf{k}$ is related to the superfluid velocity $\mathbf{v}_s$ by $\mathbf{v}_s = \hbar\mathbf{k}/m_4$, the Green's function (A37) implies a distribution function for the superfluid velocity and Eq. (A41) yields the average superfluid velocity $\langle\mathbf{v}_s\rangle_\mathbf{R}$ at space point $\mathbf{R}$.

3. Concluding remarks

We have evaluated the Green's function $G_{22} = \langle\psi\psi^*\rangle$ only for equal times $t' = t$. However, it is possible to evaluate this Green's function also for $t' \neq t$. To do this we apply the formula (A10) to the factor $e^{\alpha A} e^{\beta B}$ in Eq. (A8). The eventual result is again an integral over a single variable α with, however, a somewhat more complicated integrand than Eq. (A28). Furthermore, the nondiagonal Green's function $G_{12} = \langle\tilde{\psi}\psi\rangle$ can be calculated. In this case there is only one inverse operator L^{-1} which implies only one integral over α. This integral is performed trivially by a delta function analogous to Eq. (A9) so that eventually there will be no integral at all. The other nondiagonal Green's function $G_{21} = G_{12}^+$ is just the Hermitian conjugate. Finally, the upper-left diagonal element G_{11} is zero. Thus we conclude that the complete matrix Green's function G defined by Eq. (3.18) can be evaluated explicitly, supposed the parameters r_1 and Δr are linear functions of the space variable $\mathbf{r}$ according to Eqs. (A12) and (A13).

[1] G. Ahlers, Phys. Rev. **171**, 275 (1968).

[2] A. Onuki, J. Low Temp. Phys. **50**, 433 (1983); **55**, 309 (1984).

[3] R. Hausmann and V. Dohm, Phys. Rev. Lett. **67**, 3404 (1991); Z. Phys. B **87**, 229 (1992).

[4] R. Haussmann and V. Dohm, Phys. Rev. B **46**, 6361 (1992).

[5] R. V. Duncan, G. Ahlers, and V. Steinberg, Phys. Rev. Lett. **60**, 1522 (1988).

[6] F. C. Liu and G. Ahlers, Phys. Rev. Lett. **76**, 1300 (1996).

[7] W. A. Moeur, P. K. Day, F. C. Liu, S. T. P. Boyd, M. J. Adriaans, and R. V. Duncan, Phys. Rev. Lett. **78**, 2421 (1997).

[8] D. Murphy and H. Meyer, Phys. Rev. B **57**, 536 (1998).

[9] K. D. Erben and F. Pobell, Phys. Lett. **26A**, 368 (1968).

[10] P. Leiderer and F. Pobell, Z. Phys. **223**, 378 (1969).

[11] S. M. Bhagat and R. A. Lasken, Phys. Rev. A **3**, 340 (1971).

[12] B. I. Halperin, P. C. Hohenberg, and E. D. Siggia, Phys. Rev. Lett. **32**, 1289 (1974); Phys. Rev. B **13**, 1299 (1976).

[13] V. Dohm, Z. Phys. B **60**, 61 (1985); **61**, 193 (1985); Phys. Rev. B **44**, 2697 (1991).

[14] L. D. Landau, J. Phys. (Moscow) **5**, 71 (1941); in *Collected papers of L. D. Landau*, edited by D. ter Haar (Gordon and Breach, New York, 1965), p. 301.

[15] C. J. Gorter and J. H. Mellink, Physica (Amsterdam) **15**, 285 (1949).

[16] W. F. Vinen, Proc. R. Soc. London, Ser. A **240**, 114 (1957); **240**, 128 (1957); **242**, 493 (1957); **243**, 400 (1958).

[17] H. Baddar, G. Ahlers, K. Kuehn, and H. Fu (private communication).

[18] A. L. Fetter and J. D. Walecka, *Quantum Theory of Many-Particle Systems* (McGraw-Hill, New York, 1971).

[19] R. Hausmann, J. Low Temp. Phys. **114**, 1 (1998).

[20] H. K. Janssen, Z. Phys. B **23**, 377 (1976); C. de Dominicis, J. Phys. (Paris) **37**, C-247 (1976).

[21] P. C. Martin, E. D. Siggia, and H. A. Rose, Phys. Rev. A **8**, 423 (1973).

[22] J. M. Luttinger and J. C. Ward, Phys. Rev. **118**, 1417 (1960).

[23] C. De Dominicis and P. C. Martin, J. Math. Phys. **5**, 14 (1964); **5**, 31 (1964).

[24] A. A. Abrikosov, L. P. Gorkov, and I. E. Dzyaloshinskii, *Methods of Quantum Field Theory in Statistical Physics* (Dover, New York, 1963).

[25] G. Baym and L. P. Kadanoff, Phys. Rev. **124**, 287 (1961).

[26] G. Baym, Phys. Rev. **127**, 1391 (1962).

[27] D. J. Amit, *Field Theory, the Renormalization Group, and Critical Phenomena* (McGraw-Hill, New York, 1978).

[28] R. Haussmann, Phys. Rev. B **53**, 7357 (1996); **56**, 9684 (1997).

[29] R. Haussmann, *Self-Consistent Quantum-Field Theory and Bosonization for Strongly Correlated Electron Systems*, Lecture Notes in Physics Vol. M56 (Springer, Berlin 1999).

[30] R. Schloms and V. Dohm, Nucl. Phys. B **328**, 639 (1989).

[31] W. Y. Tam and G. Ahlers, Phys. Rev. B **32**, 5932 (1985).

[32] J. A. Lipa, D. R. Swanson, J. A. Nissen, T. C. P. Chui, and U. E. Israelsson, Phys. Rev. Lett. **76**, 944 (1996).

[33] P. K. Day, W. A. Moeur, S. S. McCready, D. A. Sergatskov, F. C. Liu, and R. V. Duncan, Phys. Rev. Lett. **81**, 2474 (1998).

[34] The DYNAMX experiment of the NASA Microgravity Fundamental Physics Program.

[35] A. Onuki, Jpn. J. Appl. Phys., Part 1 **26**, 365 (1987); J. Low Temp. Phys. **104**, 133 (1996).

[36] G. Ahlers and F. C. Liu, J. Low Temp. Phys. **105**, 255 (1996).

[37] R. Haussmann and V. Dohm, Phys. Rev. Lett. **72**, 3060 (1994); **77**, 980 (1996); Czech. J. Phys. **46**, 171 (1996).

[38] A. W. Harter, R. A. M. Lee, T. C. P. Chui, and D. L. Goodstein (private communication).

[39] K. W. Schwarz, Phys. Rev. B **18**, 245 (1978).

[40] D. F. Brewer and D. O. Edwards, Philos. Mag. **7**, 721 (1962).

[41] J. T. Tough, Prog. Low Temp. Phys. **VIII**, 133 (1982).

[42] H. E. Hall and W. F. Vinen, Proc. R. Soc. London, Ser. A **238**, 204 (1956); **238**, 215 (1956).

[43] C. F. Barenghi, R. J. Donnelly, and W. F. Vinen, J. Low Temp. Phys. **52**, 189 (1983).

[44] R. Haussmann, Z. Phys. B **87**, 247 (1992).

[45] R. Haussmann, following paper, Phys. Rev. B **60**, 12 373 (1999).

[46] T. C. P. Chui, D. L. Goodstein, A. W. Harter, and R. Mukhopadhyay, Phys. Rev. Lett. **77**, 1793 (1996).